International Journal of Earth Sciences (2024) 113:2023–2041
https://doi.org/10.1007/s00531-024-02477-9

ORIGINAL PAPER

Protracted carbon burial following the Early Jurassic Toarcian Oceanic Anoxic Event (Posidonia Shale, Lower Saxony Basin, Germany)

R. F. S. Celestino[1] · M. Ruhl[2,3] · A. J. Dickson[3,4] · E. Idiz[3] · H. C. Jenkyns[3] · M. J. Leng[5] · E. Mattioli[6] · D. Minisini[7,8] · S. P. Hesselbo[1]

Received: 2 August 2023 / Accepted: 16 October 2024 / Published online: 29 November 2024

Abstract

Lower Jurassic marine basins across the northwest European epicontinental shelf were commonly marked by deposition of organic-rich black shales. Organic-carbon burial was particularly widespread during the Toarcian Oceanic Anoxic Event (T-OAE: also known as the Jenkyns Event) with its accompanying negative carbon-isotope excursion (nCIE). Lower Toarcian black shales in central and southern Germany are known as the Posidonia Shale Formation (Posidonienschiefer) and are thought to have formed during the T-OAE nCIE. Here, we present stratigraphic (carbon-isotope, Rock–Eval, calcareous nannofossil) data from the upper Pliensbachian and lower Toarcian strata from a core drilled on the northern flank of the Lower Saxony Basin, north–west Germany. The bio- and chemostratigraphic framework presented demonstrates that (i) the rock record of the T-OAE at the studied locality registered highly condensed sedimentation and/or multiple hiatuses and (ii) the deposition of organic-rich black shale extended significantly beyond the level of the T-OAE, thereby contrasting with well-studied sections of the Posidonia Shale in southern Germany but showing similarities with geographically nearby basins such as the Paris Basin (France). Prolonged and enhanced organic-carbon burial represents a negative feedback mechanism in the Earth system, with locally continued environmental perturbance accelerating the recovery of the global climate from T-OAE-associated hyperthermal conditions, whilst also accelerating a return to more positive $\delta^{13}C$ values in global exogenic carbon pools.

Keywords Posidonia Shale · Toarcian · Black shale · Lower Saxony Basin

Introduction

The early Toarcian was characterized by major environmental changes, most notably the geographically widespread development of marine anoxia, such that this time-interval is commonly taken to record the so-called Toarcian Oceanic Anoxic Event (T-OAE or Jenkyns Events (Gambacorta et al. 2024)). The development of globally widespread marine (and lacustrine) anoxia was expressed by the formation of organic-rich, commonly laminated black shales in interconnected but hydrographically restricted sub-basins across the Laurasian Seaway of

✉ M. Ruhl
micha.ruhl@tcd.ie

✉ S. P. Hesselbo
s.p.hesselbo@exeter.ac.uk

[1] Camborne School of Mines and Environment and Sustainability Institute, University of Exeter, Penryn Campus, Treliever Road, Penryn, COR TR10 9FE, UK

[2] Department of Geology, School of Natural Sciences, Trinity College Dublin, The University of Dublin, College Green, Dublin, Ireland

[3] Department of Earth Sciences, University of Oxford, Oxford OX1 3AN, UK

[4] Centre of Climate, Ocean and Atmosphere, Department of Earth Sciences, Royal Holloway University of London, Egham, SRY TW20 0EX, UK

[5] National Environmental Isotope Facility, British Geological Survey, Nottingham, UK

[6] Université Claude Bernard Lyon 1, ENS de Lyon, UCBL, ENSL, UJM, CNRS, LGL-TPE, 69622 Villeurbanne, France

[7] ExxonMobil, 22777 Springwoods Village Pkwy, Spring, TX 77389, USA

[8] Department of Earth, Environmental, and Planetary Sciences, Rice University, 6100 Main St, Houston, TX 77005, USA

epicontinental northern Europe during the Early Jurassic. The characteristic facies include the Posidonia Shale in southern Germany, the Jet Rock in the Cleveland Basin (Yorkshire, UK) and the Schistes Carton in the Paris Basin (France) (Fig. 1) (Jenkyns 1988, 2010; Ziegler 1992; Röhl et al. 2001; Hesselbo et al. 2000; Schmid-Röhl et al. 2002, 2003; Frimmel et al. 2004; Cohen et al. 2004; Schwark and Frimmel 2004; Hermoso et al. 2009, 2013; Xu et al. 2017; Kemp et al. 2022a, b; Gambacorta et al. 2024).

The Toarcian OAE is globally associated with a − 4‰ to − 8‰ negative carbon-isotope excursion (CIE), recorded in organic and inorganic, marine and terrestrial substrates from geographically widespread locations (e.g., Jenkyns and Clayton 1987; Jenkyns 1988; Harries and Little 1999; Hesselbo et al. 2000; McArthur et al. 2000; Röhl et al. 2001; van Breugel et al. 2006; Hesselbo et al. 2007; Woodfine et al. 2008; Sabatino et al. 2009, 2013; Al-Suwaidi et al. 2010; Caruthers et al. 2011; Kafousia et al. 2011; Kemp and Izumi 2014; Them et al. 2017; Xu et al. 2017, 2018a; Fantasia et al. 2019; Baghli et al. 2020; Ullmann et al. 2020; Al-Suwaidi et al. 2022; Bodin et al. 2023; Storm et al. 2024). The characteristic T-OAE negative carbon-isotope excursion (CIE) likely resulted from the massive injection of isotopically light (^{12}C enriched) carbon into the ocean–atmosphere system from magma degassing linked to Karoo-Ferrar Large Igneous Province (LIP) emplacement, and/or the release of thermogenic methane from sill-intruded subsurface organic-rich sediments in the Karoo Basin, and/or the dissociation of sub-seafloor methane clathrates (Hesselbo et al. 2000; McElwain et al. 2005; Svensen et al. 2007; Percival et al. 2015; Jones et al. 2016; Heimdal et al. 2021; Ruhl et al. 2022). The associated perturbations to the global carbon cycle resulted in climatic, environmental and biotic/ecosystem changes, such as significant global warming (characterizing this event as a hyperthermal), an accelerated hydrological cycle (leading to enhanced global continental weathering rates), the widespread development of anoxic conditions, and a major extinction event (Jenkyns 1985; Harries and Little 1999; McArthur et al. 2000; Röhl et al. 2001; Bailey et al. 2003; Cohen et al. 2004; Hesselbo et al. 2007; Gómez et al. 2008; Mattioli et al. 2009; Sabatino et al. 2009; Al-Suwaidi et al. 2010; Hesselbo and Pienkowski 2011; Caswell and Coe 2014; Ikeda and Hori 2014; Percival et al. 2016; Them et al. 2017; Dickson et al. 2017; Xu et al. 2017, 2018a; Fantasia et al. 2018; Ruebsam et al. 2020; Ullmann et al. 2020; Erba et al. 2022; Kemp et al. 2022a, b). The T-OAE was preceded by a smaller carbon-cycle perturbation at the Pliensbachian–Toarcian boundary, which was probably linked to early phases of volcanic activity within the Karoo-Ferrar LIP region, as shown by sedimentary Hg enrichment, magnetostratigraphy, and U–Pb radio-isotopic dating, suggesting that volcanic activity was initiated in the late Pliensbachian (Hesselbo et al. 2007; Littler et al. 2010; Percival et al. 2015; Bodin et al. 2016; Xu et al. 2018b; De Lena et al. 2019; Al-Suwaidi et al. 2022; Ruhl et al. 2022).

One of the organic-rich sedimentary units associated with the development of anoxia in basins of the Laurasian Seaway was the Posidonia Shale Formation (Posidonienschiefer), which crops out in Southern Germany and is present in the subsurface of northern Germany and the western Netherlands (Küspert 1982; Riegraf et al. 1984; Littke et al. 1991; Ziegler 1992; Röhl et al. 2001; Schmid-Röhl et al. 2002; Frimmel et al. 2004; Schwark and Frimmel 2004; Montero-Serrano et al. 2015; Song et al. 2017). Studies conducted across different NW European basins, show that the expression of the T-OAE differs between localities, suggesting a strong local/regional control on the depositional environment, superimposed on global climatic and environmental perturbances (e.g., Remirez and Algeo 2020a and b and references therein). Within Germany, most studies on the T-OAE, integrating high-resolution carbon-isotope stratigraphy and biostratigraphy, have focused on the SW German Basin, with few detailed stratigraphic datasets available from the Lower Saxony Basin. We present here a high-resolution carbon-isotope dataset combined with calcareous nannofossil biostratigraphy, pyrolysis, and sedimentological data obtained from a core drilled in the Lower Saxony Basin (LSB) of NW Germany. The studied succession stratigraphically covers the Posidonia Shale Formation and the T-OAE interval. With this framework, we characterize the lithostratigraphic expression of the T-OAE and the Pliensbachian–Toarcian boundary event in the LSB, suggest stratigraphic correlation to well-documented reference sections elsewhere, and provide evidence for the stratigraphic diachroneity of Posidonia Shale successions between adjacent basins. Our objective is to differentiate and constrain the timing of the depositional mechanisms leading to the formation of organic-rich black shales in geographically separated, but locally adjacent basins during the T-OAE.

Regional geological setting

The Lower Saxony Basin (LSB) (Fig. 1) is an E–W-trending 350-km-long and 100-km-wide basin that developed through extension and subsidence during the breakup of the supercontinent Pangaea (Betz et al. 1987; Brink et al. 1992; Ziegler 1992; Senglaub et al. 2005; Bruns et al. 2013). Thickness variations of the sedimentary units in the LSB, identified through seismic reflection profiles and well-data, suggest that the basin formed initially as a large, asymmetric, and internally faulted graben system (Bruns et al. 2013). The Jurassic sediments of the LSB are composed of calcareous claystone, limestone,

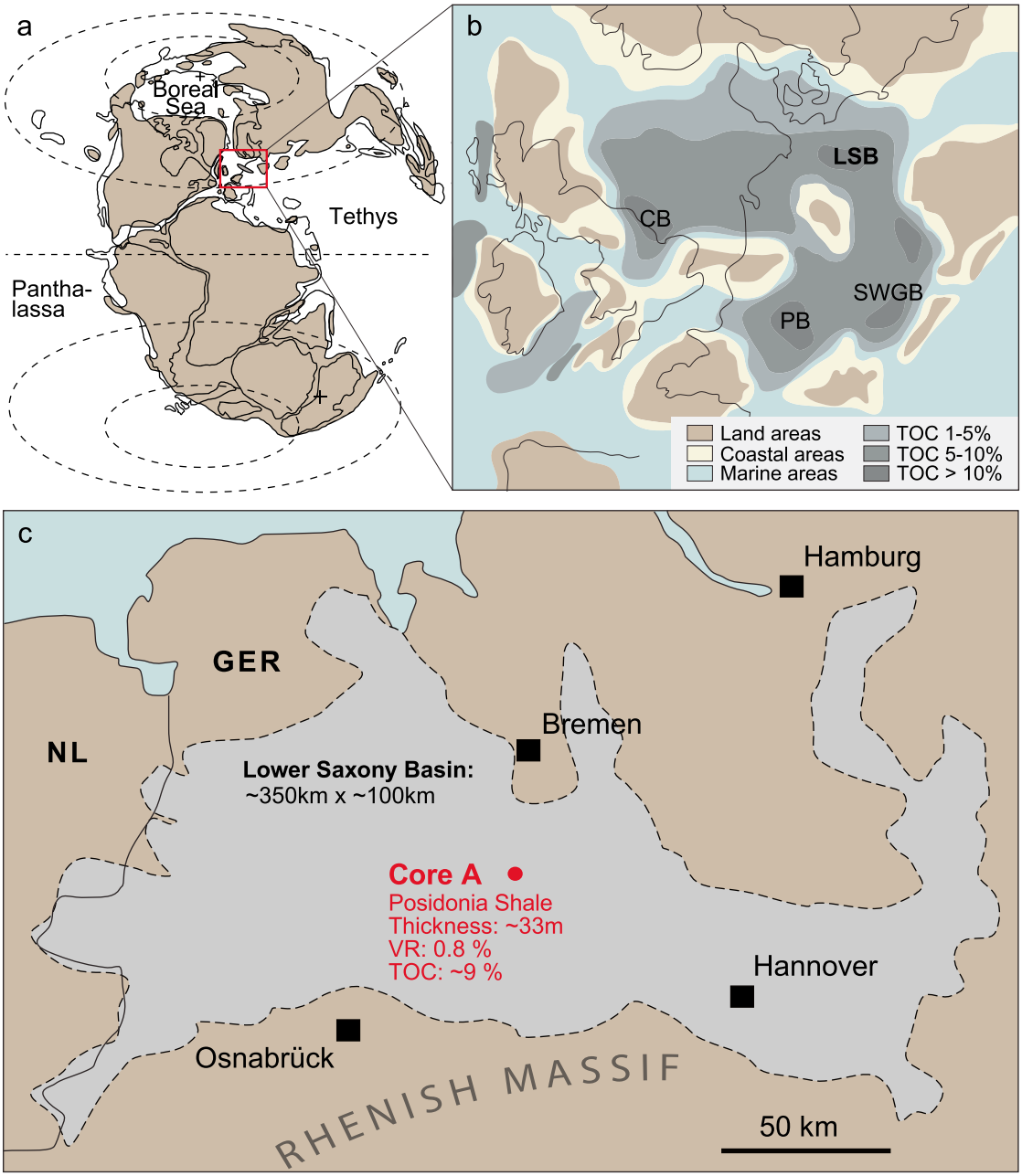

Fig. 1 **a** Early Jurassic palaeogeography. **b** Palaeogeographic location of Lower Saxony Basin (LSB), and nearby basins marked by total organic carbon (TOC) accumulation in the Laurasian Seaway. *CB* Cleveland Basin; *PB* Paris Basin; *SWGB* Southwest Germanic Basin; *LSB* Lower Saxony Basin (modified after Korte et al. 2015; Ruebsam et al. 2018). **c** Geographical map of NW Germany showing the extent of the Lower Saxony Basin in the subsurface (modified after Betz et al. (1987)), with marked the geographic location of the here-studied Core A

sandstone, and shale. The eastern part of the basin was dominated by a shallow-water deltaic depositional environment, with sandy deposits, while the western part was characterized by deeper water shales and marls, including the organic-rich Toarcian Posidonia Shale Formation (Fig. 1) (Senglaub et al. 2005). The thickness of the Posidonia Shale Formation varies between 25 and 70 m across the basin because of spatially varying sedimentation rates and/or stratigraphic variation in hiatuses at its base and top. Across the LSB, the Posidonia Shale reached varying burial depths, with current burial depths of 1–3 km, but possibly as much as 3–8 km during the Early Cretaceous, with resultant degradation of sedimentary organic matter, hydrocarbon formation and expulsion, and formation

of 'beef' calcite veins (McCann 2008; Bruns et al. 2013; Hooker et al. 2020; Dickson et al. 2022).

Materials and methods

Materials

The samples studied here from an industry core, Core A, in the Lower Saxony Basin (LSB) span a ~ 70 m stratigraphic interval (Fig. 1). Sediments in Core A are thermally immature and present the most complete and expanded upper Pliensbachian and Toarcian sedimentary succession of the LSB, thereby arguably presenting the best reference core for the Posidonia Shale. Core A is referred to as Well A in Gorbanenko and Ligouis (2014), Core A in Dickson et al. (2022), and Core 1 in Hooker et al. (2020).

Bulk organic $\delta^{13}C$ analysis

The carbon-isotope composition ($\delta^{13}C$) of total sedimentary organic carbon was measured on 340 decarbonated bulk-rock samples, which were crushed and ground to a fine powder using an agate pestle and mortar. An aliquot of ~ 0.5 g was weighed in to 50-ml centrifuge tubes, and 10% hydrochloric acid was added and the resultant mixture subsequently heated to 60 °C in a water bath. The samples were then rinsed three times with distilled water and dried in an oven at 40 °C. Between 5 and 100 mg of decarbonated sediment, depending on organic-carbon content, was weighed into tin capsules to be measured for $\delta^{13}C$. $^{13}C/^{12}C$ analyses were performed by combustion in a Costech ECS4010 Elemental Analyser (EA) online to a VG TripleTrap and Optima dual-inlet mass-spectrometer at the British Geological Survey, Keyworth (UK). The $\delta^{13}C$ values were calibrated to V-PDB, using a within-run laboratory standard calibrated against NBS18, NBS-19 and NBS-22. Replicate analysis of well-mixed samples indicated a precision of < 0.1‰ (1 SD).

Calcareous nannofossil biostratigraphy

Calcareous nannofossil identification was carried out on 59 samples from Core A, at the Université Claude Bernard, Lyon 1, France. Stratigraphic sample resolution is approximately 2 m within the Posidonia Shale Formation, and down to 10 cm around the formation boundaries and the interval covering the T-OAE. Sample positions for calcareous nannofossil biostratigraphy are shown in Fig. 2. Smear slides of rock powder (Bown and Young 1998) were mounted using Rhodopass mounting medium and then studied under an optical polarizing microscope at 1000×. All the encountered nannofossil specimens were counted along 3 transverses of the slide (3 mm^2), using an Axioskop 40 Zeiss polarizing microscope. NJT zonation after Ferreira et al. (2019), modified after Mattioli and Erba (1999) and Bown and Cooper (1998), was used. Preservation degree of nannofossils was estimated according to etching and overgrowth of specimens (Roth 1984): poor nannofossil assemblages show strong etching, overgrowth or fragmentation; moderate and good have limited alteration.

Rock–Eval pyrolysis

Between 2 and 100 mg of powdered bulk-rock samples ($n = 287$) were weighed into stainless steel crucibles and measured using a Rock–Eval 6 Unit (Behar et al. 2001), at the Department of Earth Sciences, University of Oxford. A temperature profile of 300–650 °C for pyrolysis and 300–850 °C for oxidation was applied to the samples. S1, S2, Tmax, S3, S4 and S5 peaks were determined to calculate the Hydrogen Index (HI, in mg HC/g TOC), Mineral Carbon (weight %), Oxygen Index (OI, in mg CO_2/g TOC), Residual Organic Carbon (%) and total organic carbon (TOC, %). An in-house standard SAB134 (Blue Lias, Jurassic; Hesselbo et al. 2004) was measured every ten samples through the analytical programme. One standard deviation on repeated TOC and HI analyses of the SAB134 in-house standard is 0.065% (TOC) and 22.65 mg HC/g TOC (HI), respectively.

Results

Sedimentology and lithostratigraphy

The studied sedimentary succession in Core A of the LSB covers part of the Lias delta, Lias epsilon and Lias zeta, also known as the Amaltheenton, Posidonienschiefer (Posidonia Shale) and Jurensismergel formations, respectively (Fig. 2, Supplementary Fig. 1). The Amaltheenton Formation (Fm), at the base of the studied core, is composed of quartz- and clay-rich, dark-grey mudstone with abundant sideritic nodules and pyritized burrows. The carbonate content is low through this stratigraphic interval, with only a few samples containing calcareous nannofossils; the abundant scours are filled with silt to fine sand. The transition from the Amaltheenton to the Posidonia Shale Formation is characterized by a succession of condensed horizons and carbonate-rich concretionary intervals (interpreted as hiatus concretions; cf. Voigt 1968) between 45 and 43 m in the studied succession (Figs. 2, 3a–c and 5; relative depths with respect to top of the studied interval). The first carbonate-rich unit occurs at 45 m and is composed of a 30-cm-thick network of septarian nodules with cracks filled with multiple generations of calcite (Fig. 3d), with the top showing abundant

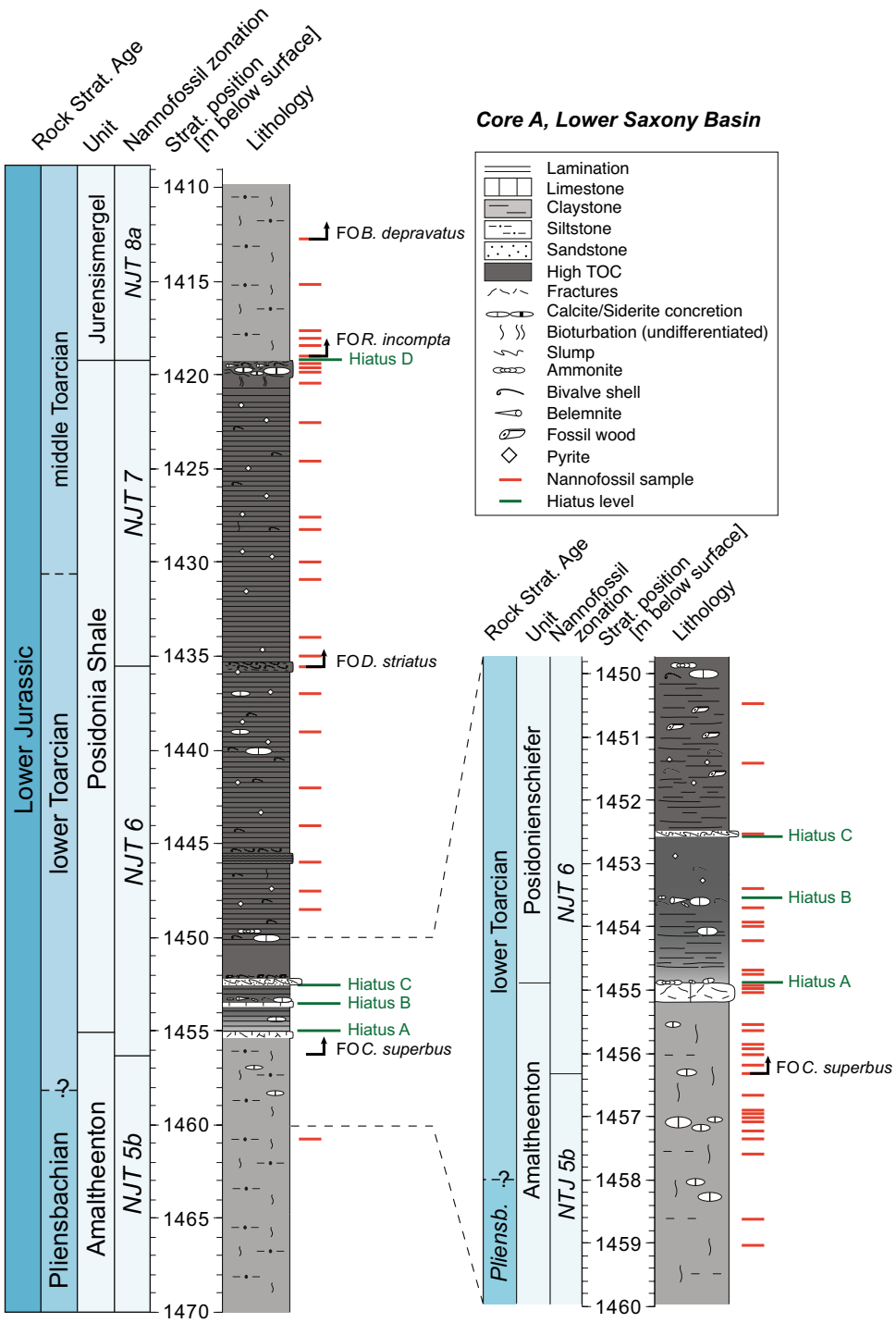

Fig. 2 Lithological log of Core A with First Occurrences of calcareous nannofossils, stratigraphic location of main hiatus horizons, and sample positions for calcareous nannofossil biostratigraphy (red lines). An enlarged view of the 40–50 m cored section highlights the more detailed sedimentology and higher resolution sampling of this interval

reworked carbonate nodules and sediment infilling of cracks at a hiatus concretion level (Fig. 3c, Hiatus A), similar to observations on the Sinemurian mudstone successions in the Wessex Basin, Dorset, UK (Hesselbo and Palmer 1992). The hiatus concretion at 45 m is taken here as the boundary between the Amaltheenton and Posidonia Shale formations and marks an upward change to overall dark-grey and dark-brown (sub-) laminated marl. Stratigraphically upward, identified nodules change from sideritic to calcitic (Fig. 3) and become abundant throughout the lower part of the Posidonia Shale.

A second level of condensed sedimentation and/or erosion is evident at 43.5 m, showing reworked calcite nodules as well as belemnite rostra and shell fragments overlying an erosional surface (Fig. 2, Hiatus B). Sediments between hiatuses A and B comprise dark grey–brown mudstone with

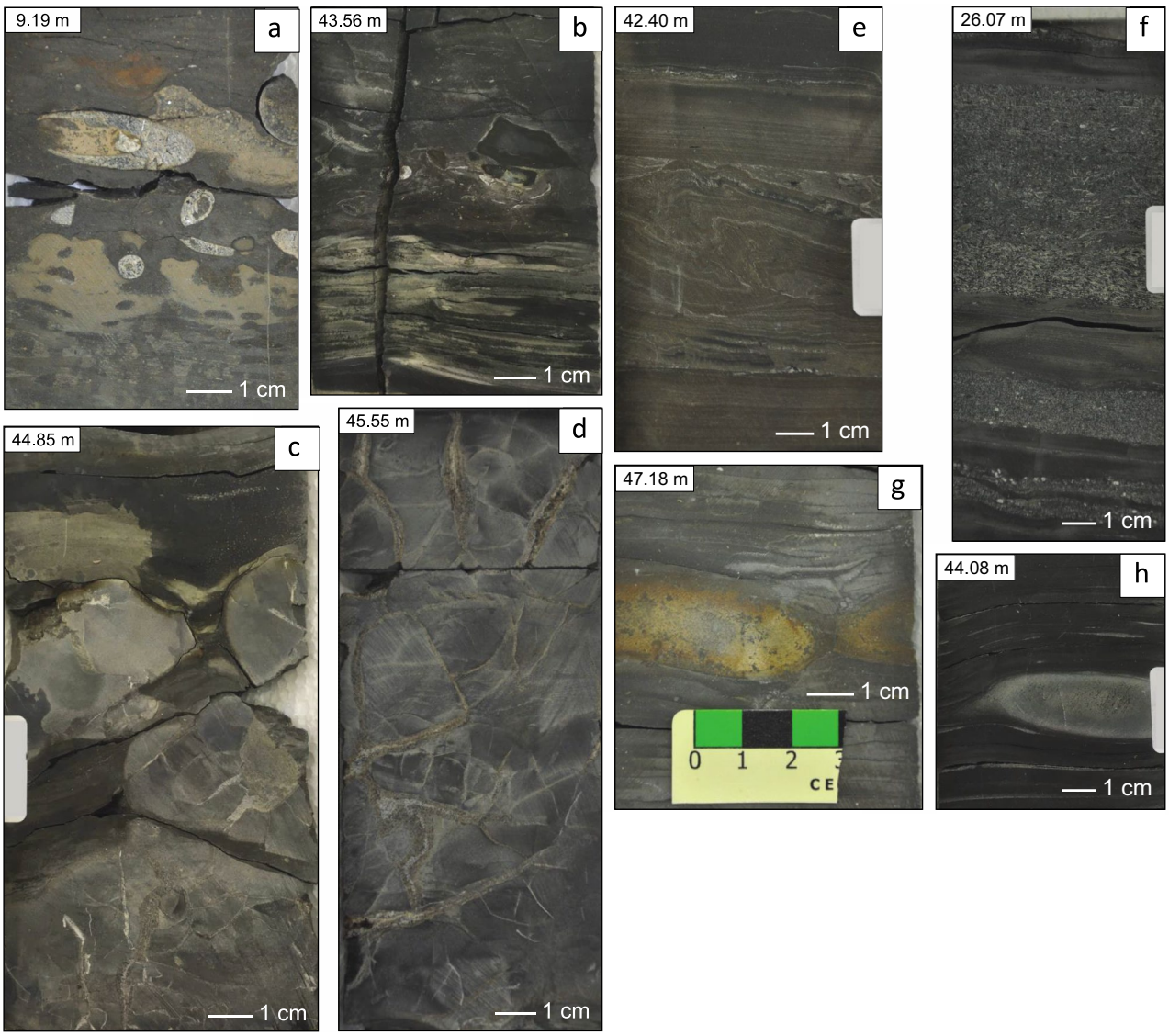

Fig. 3 Core photographs showing sedimentological features in Core A. **a** Top of the Posidonia Shale Formation showing burrowed firmground and overlying debris of belemnite rostra with microborings (Hiatus D). **b** Erosional surface on pale yellow-grey very fine sand lamina overlain by condensed stratigraphic horizon with belemnite and shell debris as well as reworked nodule fragments (Hiatus B). **c** Partially broken-up septarian carbonate nodule with sediment-filled cracks. The top shows reworked nodules (Hiatus A). **d** Septarian crack network with two phases of calcite growth. **e** Brown mudstone soft-sediment deformation with common silt and very fine sand-sized clastic and shell material with truncated base and top (Hiatus C). **f** Two horizons with very fine sand-sized clastic material, followed by a 10 cm-thick shell debris layer. **g** Siderite nodule (Amaltheenton Formation). **h** Calcareous nodule (Posidonia Shale Formation)

multiple well-defined mm-thick silty layers, suggesting episodic sediment redeposition. Between 43.5 and 42.5 m in the studied succession the dark grey–brown mudstone shows no clear lamination and contains abundant pyrite-filled burrows. From 42.6 m upwards the sedimentary facies changes with the onset of visible lamination and common horizons of silt and very fine sand and terrestrial plant debris (Fig. 3e). A 10-cm thick unit at 42.5 m shows clear soft sediment deformation, with the sharp base and top suggesting a hiatus (Fig. 3e, Hiatus C). Coarser grained (turbiditic) silty levels decrease in abundance from 41 m upwards, and the subsequent deposits to the top of the Posidonia Shale Formation are dominated by brown–grey mudstones with diffuse lamination and an absence of clearly visible bioturbation. Abundant thin-shelled bivalves, macroscopically visible pyrite, as well as small pieces of fish bone, can be found in the lower half of the formation.

Calcite concretions occur at several levels, but mostly below 26 m in the studied succession. At 26 m, a 1 cm thick layer consisting of sand-sized detrital grains, is followed by

a 10 cm-thick layer of shell debris (Fig. 3f). The upper half of the Posidonia Shale in Core A is homogenous and very poor in macrofossil material, with also only a few small burrows and varying degrees of lamination. The top of the Posidonia Shale is marked by a condensed horizon (Fig. 2, Hiatus D) containing abundant debris of belemnite rostra with microborings as well as larger burrow structures with pale-coloured sediment infill. The overlying Jurensismergel is characterized by the absence of lamination and signs of bioturbation with regular occurrence of pyrite replacement in burrow structures.

Integrated carbon-isotope and calcareous nannofossil stratigraphy

Stable bulk sedimentary organic carbon-isotope analyses of Core A, with an overall sample resolution of 5–15 cm and a ~2 cm sample resolution of the T-OAE stratigraphic interval, show values of − 25.8‰ for the lowermost part of the core (at 67–70 m in the studied succession), followed by a sharp negative shift to − 26.5‰ at 66 m, possibly indicating a hiatus in the record (Fig. 4). Values gradually increase up-section to − 26‰ at 58 m, before decreasing to ~− 29.5‰ at 48 m. The $\delta^{13}C_{TOC}$ record shows a narrow negative CIE of ~1.5‰ between 50 m and 46 m. More elevated values of ~− 28‰ at 47–44 m are subsequently followed by an abrupt negative shift in $\delta^{13}C_{TOC}$ down to − 30‰ before values are truncated and sharply increase to − 26‰ at 43 m. The $\delta^{13}C_{TOC}$ values thereafter decrease over half a metre to − 32‰ at 42.5 m, representing a negative excursion, with values subsequently increasing more gradually to − 26.5‰ at 41.5 m. From 41.5 m to 34 m in the studied section the $\delta^{13}C_{TOC}$ data show a decreasing trend to a point where values remain relatively

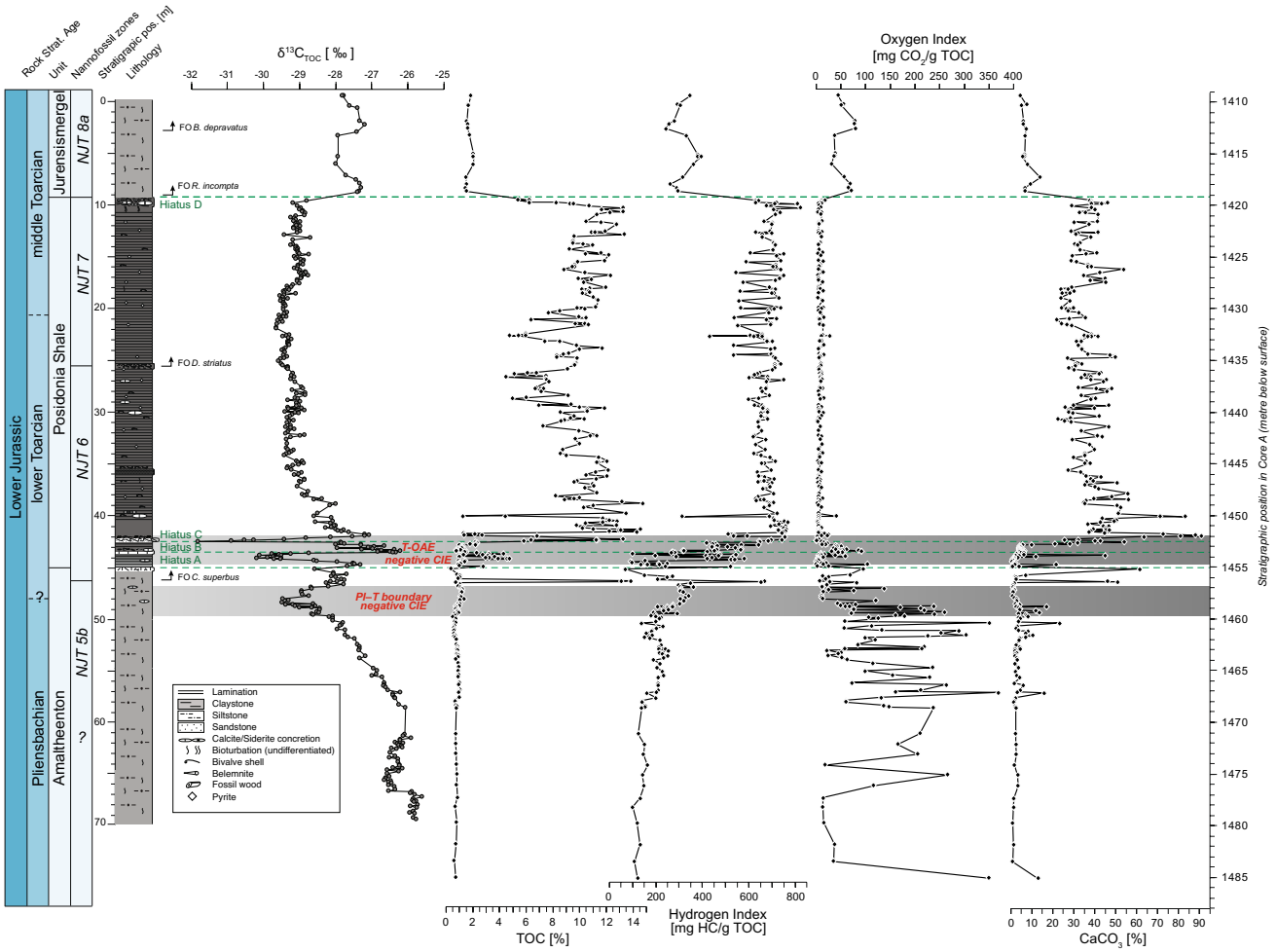

Fig. 4 Lithological log of Core A with First Occurrences of calcareous nannofossils, stratigraphic location of main hiatus horizons, and the generated $\delta^{13}C_{TOC}$ (this study), Total Organic Carbon (TOC: this study, Hooker et al. 2020; Dickson et al. 2022), Hydrogen Index (HI: this study), Oxygen Index (OI: this study) and the calculated calcium carbonate (inferred from the mineral carbon content: this study) curves with the identified Toarcian Oceanic Anoxic Event (T-OAE) and the likely stratigraphic position of the Pliensbachian–Toarcian boundary

stable at approximately − 29‰ up to 10 m, where another sharp increase in values to − 26.5‰ can be observed. The uppermost 10 m of the studied succession in the core is characterized by values of around − 27‰ to − 28‰ with only minor variation.

Calcareous nannofossil data from the same core identify Lower Jurassic biozones, and permit assignment of the boundary between the NJT5b-c Zone and the NJT6 Zone (Figs. 4, 5 and Supplementary Fig. 2), with the First Occurrence of *Carinolithus superbus* at 46 m, within the uppermost part of the Amaltheenton Formation. Samples studied from the Amaltheenton Formation generally contain very few calcareous nannofossils, whereas samples from the Posidonia Shale show abundant nannofossils from 41 m upwards. The nannofossil *Crepidolithus crassus*, typically found in the recovery phase of the T-OAE in successions elsewhere (Mattioli et al. 2008), is dominant in this interval. The First Occurrence of *Discorhabdus striatus*, at 25 m, combined with a reduced dominance of *C. crassus* and an increase of *Schizosphaerella* at this level defines the boundary between NJT6 and NJT7 in Core A. The top of the NJT7 Zone is assigned to the stratigraphic level at 9.3 m, coinciding with Hiatus D, and the formation boundary between the Posidonia Shale and the Jurensismergel. The overlying Jurensismergel is characterized by the First Occurrence of *Retecapsa incompta,* which defines the base of the NJT8a nannofossil Zone. The *Schizosphaerella* abundance decreases in the Jurensismergel, whilst larger *Lotharingius* nannofossils become more dominant. Overall, the calcareous nannofossil biostratigraphy allows assignment of the Amaltheenton Formation to the upper Pliensbachian, and the Posidonia Shale and Jurensismergel to the lower to middle Toarcian. The combined calcareous nannofossil biostratigraphy and carbon-isotope chemostratigraphy suggest the Pliensbachian–Toarcian boundary to coincide with the ~ 1.5‰ negative CIE at ~ 48 m in the studied succession of Core A. The First Occurrence of *C. superbus* and the shifts to $\delta^{13}C_{TOC}$ values of − 32‰ suggest the sedimentary succession associated with the T-OAE negative CIE to be constrained between 42 and 44.5 m in Core A, where it is truncated and/or strongly condensed.

Organic matter type

Rock-Eval pyrolysis was used to determine organic-matter content (total organic carbon: TOC) and kerogen type (hydrogen index: HI) in the studied sedimentary succession. The HI value is commonly used to evaluate the impact of possible source mixing on the bulk organic $\delta^{13}C_{TOC}$ record. Total organic carbon (TOC) content varies substantially within the studied stratigraphic interval, between 1% and 15% [this study (Fig. 4); Hooker et al. 2020; Dickson et al. 2022]. Low TOC values of ~1% characterize the Amaltheenton Formation, except for a stratigraphically short increase up to 14% TOC at ~46.5 m. Sedimentary TOC content varies between 1% and 5% in the lower 2.5 m of the Posidonia Shale, followed by a significant rise to 13% TOC at the stratigraphic level of Hiatus C (Fig. 4). The TOC content subsequently remains generally high, between 5% and 15% throughout the remainder of the Posidonia Shale. TOC concentrations significantly reduce again to ~1% at Hiatus D, the boundary between the Posidonia Shale and overlying Jurensismergel Formation.

Hydrogen index values generally mimic the TOC record, with values of 100–300 mg HC/gTOC in the Amaltheenton Formation and 500–800 mg HC/gTOC in the Posidonia Shale (Figs. 4 and 6). High HI and low oxygen index (OI) in the Posidonia Shale suggest a well-preserved, elevated marine algal contribution to the bulk sedimentary organic matter. Hence, small variations in HI and OI in the main body of the Posidonia Shale possibly reflect minor changes in the relative contribution of pelagic algal marine organic matter *vs* terrestrial organic matter. The generally poor correlation between $\delta^{13}C_{TOC}$ and HI values in the studied succession of Core A (Fig. 6) suggests that changes in organic-matter source were not the main driver of stratigraphic changes in bulk organic carbon-isotope values.

Discussion

Protracted deposition of the posidonienschiefer after the T-OAE

The Lower Saxony Basin is one of the main basins of the north European epicontinental seaway. Compared to the well-studied Toarcian records of the Southern German Basin (e.g., Röhl et al. 2001; Schmid-Röhl et al. 2002; Schwark and Frimmel 2004), to date only limited Lower Jurassic bio- and carbon-isotope stratigraphic data exist for the Lower Saxony Basin (e.g., Gorbanenko and Ligouis 2014; Gorbanenko 2015; van de Schootbrugge et al. 2019; Marten et al. 2024; Schwark and Ruebsam 2024), with much data originating from the Hils Syncline (e.g., Vandenbroucke et al. 1993, and references therein). Comparison of the geographic and stratigraphic variation in geochemical, physical, and biological characteristics of the Posidonia Shale within and between the LSB and adjacent basins provides constraints on the mechanisms leading to the intra- and inter-basinal variation in organic-carbon burial and deposition of black shale in the Laurasian seaway during the Toarcian.

Many of the well-studied sections and cores in NW Europe and elsewhere, covering the T-OAE interval, show organic-carbon enrichment predominantly during the T-OAE negative CIE stratigraphic interval (e.g., Jenkyns et al. 2002; Kemp et al. 2005; Hesselbo et al. 2007; Xu et al. 2018a; Erba

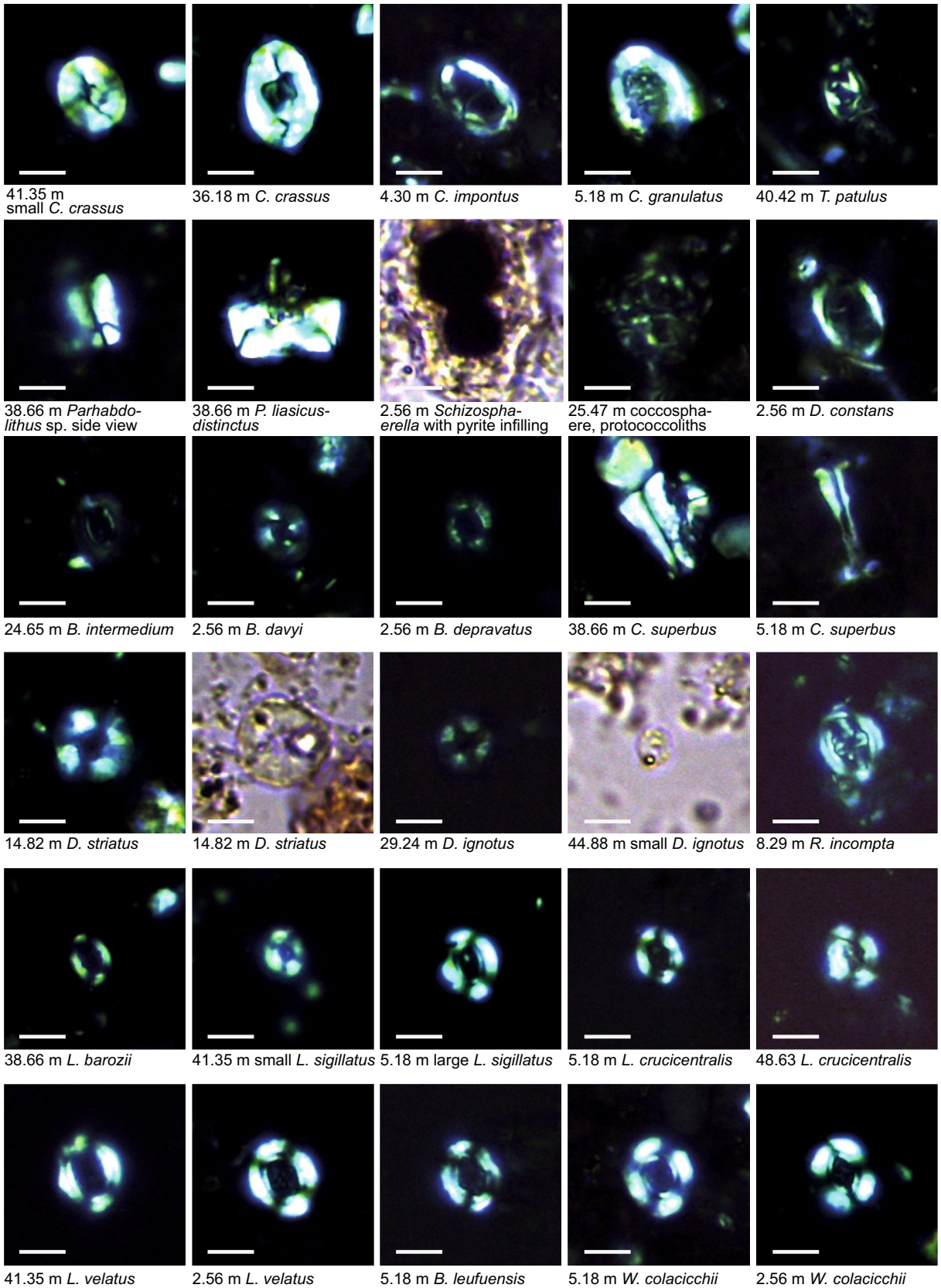

Fig. 5 Selection of the most important calcareous nannofossils identified in Core A. Images with black background were taken with cross-polarized light and the white scale is 5 µm

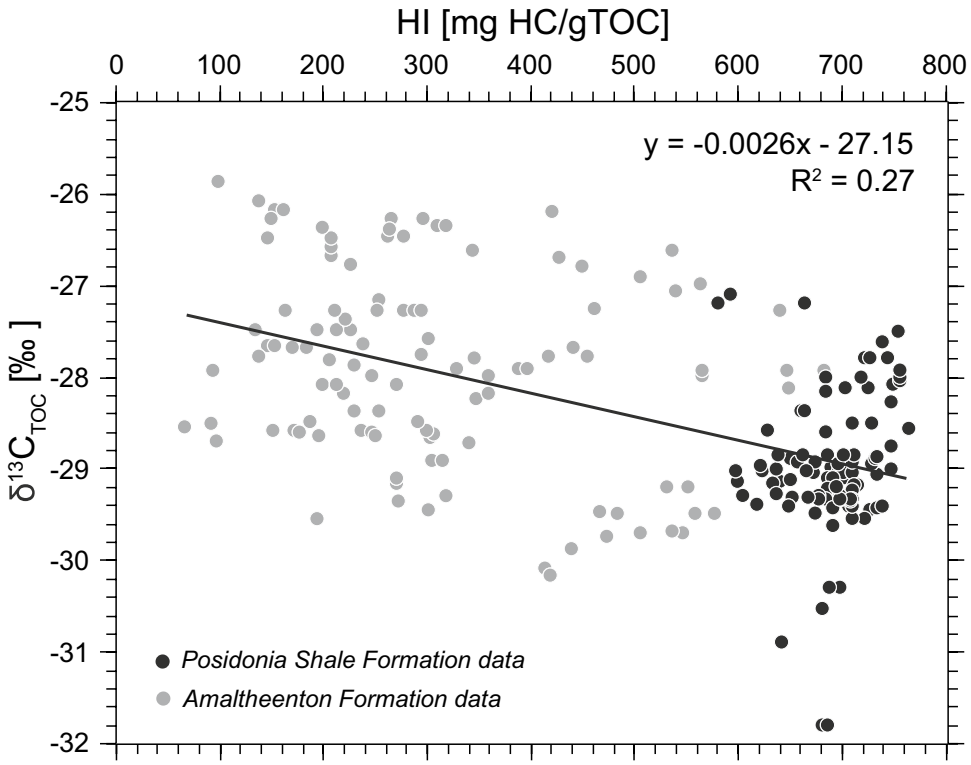

Fig. 6 Cross-plot of $\delta^{13}C_{TOC}$ and corresponding Hydrogen Index (HI) showing the absence of a strong correlation, suggesting that stratigraphic variations in $\delta^{13}C_{TOC}$ occur independently from organic-carbon source mixing, but rather because of exogenic carbon cycle changes at that time. Amaltheenton Formation data in grey; Posidonia Shale Formation data in black

et al. 2022; Kemp et al. 2022a, b). Integrated calcareous nannofossil, carbon-isotope and lithostratigraphic analyses of Core A enabled correlation to sections elsewhere, including the expanded reference section of the Llanbedr (Mochras Farm) borehole, Cardigan Bay Basin (UK), hereafter referred to as Mochras, providing the first detailed stratigraphic framework for the upper Pliensbachian and Toarcian sediments of the Lower Saxony Basin (Germany). Stratigraphical age assignment in the Lower Saxony Basin is, however, challenging for the Amaltheenton Formation, e.g., particularly below 50 m in Core A, as this part of the core does not contain sufficient calcareous nannofossils to establish a nannofossil zonation. The first nannofossil Zone to be reliably determined is NJT5b-c, based on the concomitant presence of *Lotharingius crucicentralis*, *Lotharingius velatus*, *Etmorhabdus crucifer* and *Discorhabdus ignotus*. Such a nannofossil assemblage in this stratigraphic interval suggests an age at around the Pliensbachian–Toarcian boundary as these species have their First Occurrence very close to the base of the Toarcian in stratigraphically well-constrained sections (Supplementary Fig. 2) (Bucefalo Palliani and Mattioli 1998; Mattioli and Erba 1999; Mattioli et al. 2013; Fraguas et al. 2015; Menini et al. 2018; Ferreira et al. 2019). At the same stratigraphic level, the $\delta^{13}C_{TOC}$ signal shows a small-amplitude negative excursion, which is tentatively interpreted to record the Pliensbachian–Toarcian boundary event (cf. Hesselbo et al. 2007; Littler et al. 2010; Da Rocha et al. 2016; Xu et al. 2018a).

Stratigraphic correlation between the upper Pliensbachian strata in Core A, with the Sancerre core of the Paris Basin, which includes a high-resolution calcareous nannofossil biostratigraphic zonation (Peti et al. 2017) and the Schandelah core from the Lower Saxony Basin (van de Schootbrugge et al. 2019) is challenging due to the lack of a characteristic and easily identifiable carbon-isotope event during this time period. The stratigraphically lowest large-amplitude excursion in the $\delta^{13}C_{TOC}$ record of the Sancerre core is a negative shift close to the top of the *P. margaritatus* ammonite Zone, which is also observed in both the Schandelah and Mochras cores (Peti et al. 2017; van de Schootbrugge et al. 2019; Storm et al. 2020). As no large amplitude $\delta^{13}C_{TOC}$ negative shift is visible in Core A of the Lower Saxony Basin, a substantial hiatus is inferred (Hiatus A?), and the lowermost part of the core tentatively assigned to the NJT5b, NJT5a and NJT4b nannofossil zones, corresponding to the time period equivalent to the *A. margaritatus* and upper *P. spinatum* ammonite zones. A similar pattern of truncation of upper Pliensbachian strata is inferred from carbon-isotope stratigraphy in other basins (Bodin et al. 2023).

Above the assigned Pliensbachian–Toarcian boundary at 48 m, a gradual change to more positive $\delta^{13}C_{TOC}$ values can be observed, reaching − 26‰ at the transition between the Amaltheenton and the Posidonia Shale, representative of an overall positive excursion up to 35 m. This overall positive excursion is interrupted by two negative shifts of − 3‰ and − 7‰, respectively, with the latter falling to

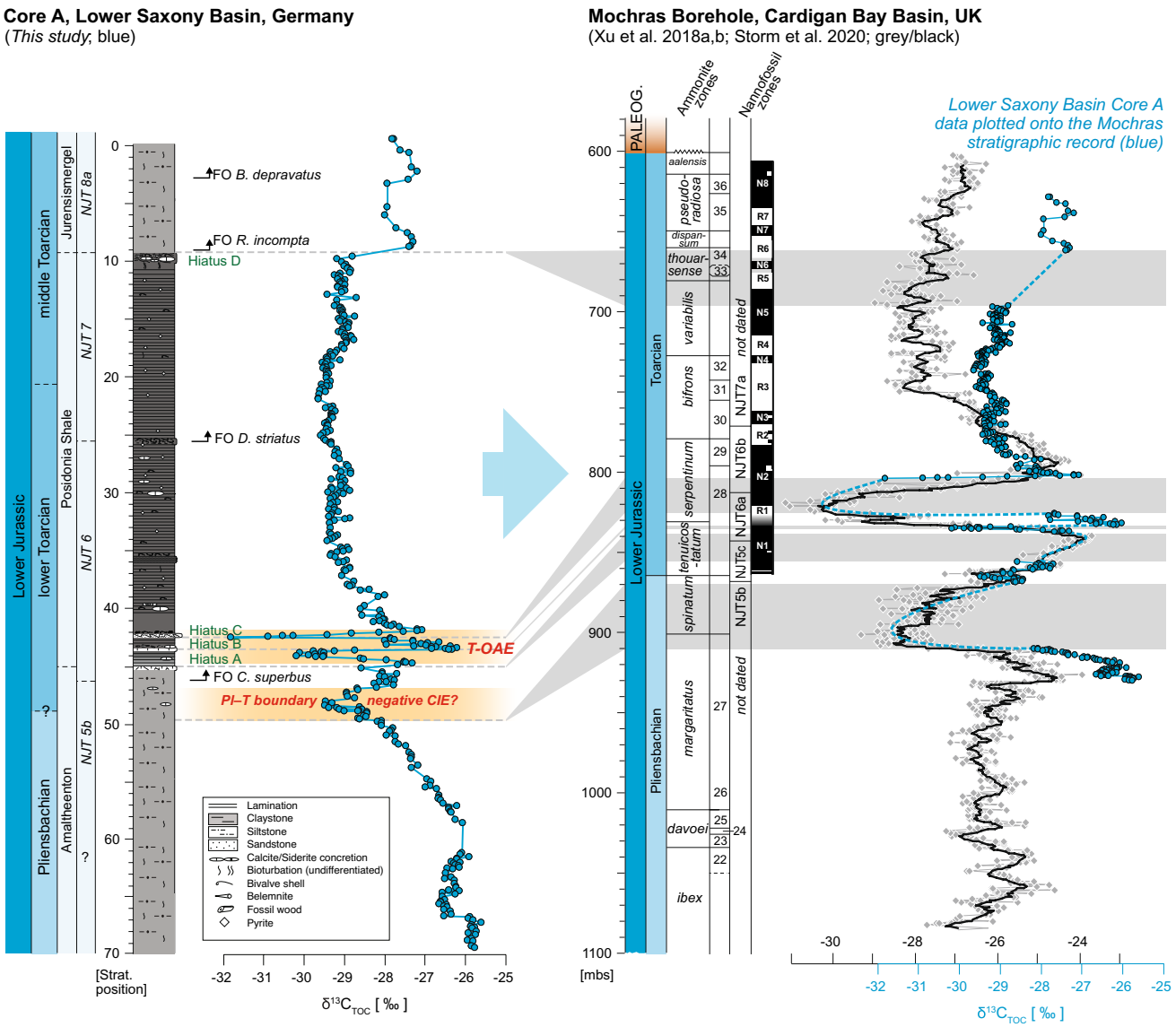

Fig. 7 Integrated stratigraphic record for Core A, with the d.$^{13}C_{TOC}$ record from Core A, superimposed on the stratigraphic record of the Mochras core. Ammonite zonation from Ivimey-Cook (1971), Page in Copestake and Johnston (2013) and Pieńkowski et al. (2024); carbon isotopes and magnetostratigraphy from Xu et al. (2018a,b) and (Storm et al. 2020); nannofossil zonation from Ferreira et al. (2019)

values of − 32‰. This positive excursion, with the superimposed ~− 7‰ negative shift, is here taken as the chemostratigraphic signature of the Toarcian Oceanic Anoxic Event (T-OAE). These two observed negative excursions in $\delta^{13}C_{TOC}$ are separated by even more positive $\delta^{13}C_{TOC}$ values and may reflect the stepped $\delta^{13}C_{TOC}$ record typical for the onset of the T-OAE negative carbon-isotope excursion (CIE), albeit probably intersected by multiple hiatuses. The overall condensed nature of this stratigraphic interval in the Lower Saxony Basin, combined with the occurrence of stratigraphic hiatuses and the lack of ammonite biostratigraphy, challenges correlation of specific steps in the $\delta^{13}C_{TOC}$ record to time-equivalent strata in sedimentary archives at other localities. Nevertheless, the recognition of the T-OAE in this part of the core, based on the occurrence of very negative carbon-isotope values, superimposed on an overall long-term positive CIE is supported by nannofossil biostratigraphy. The First Occurrence of the nannofossil *C. superbus* at 46 m assigns the overlying stratigraphic interval to the NJT6 Zone (Ferreira et al. 2019).

The NJT6 Zone encapsulates the negative carbon-isotope excursion and TOC maximum characterizing the T-OAE in many Tethyan sections and In the Euro-Boreal domain (e.g., Mattioli et al. 2004; Menini et al. 2018, 2021; Ferreira et al. 2019), the *C. superbus* nannofossil Zone is thus proven to be reliable for inter-regional correlations. In the Euro-Boreal

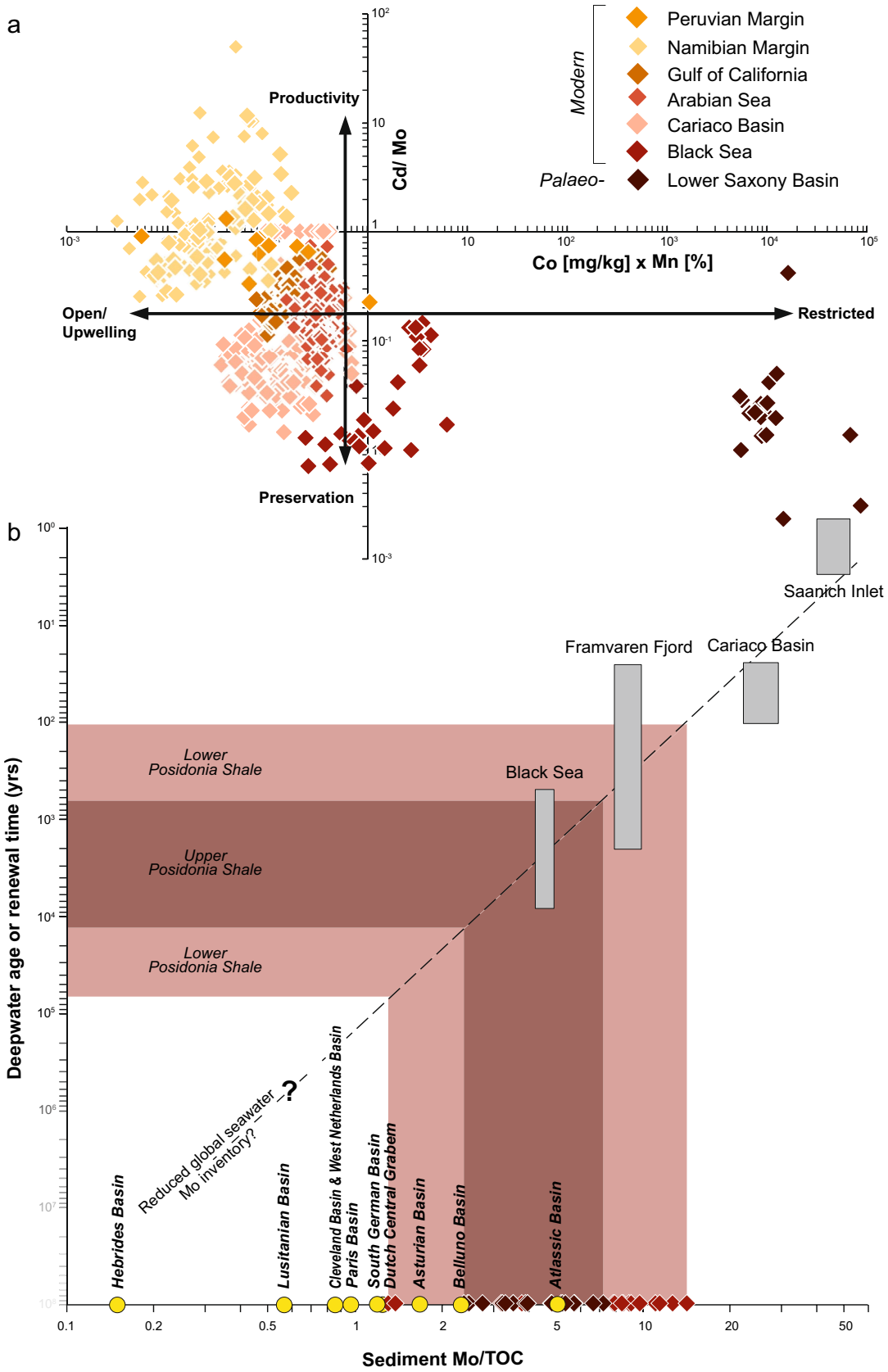
a
Peruvian Margin
Namibian Margin
Gulf of California
Arabian Sea
Cariaco Basin
Black Sea
Lower Saxony Basin
Modern
Palaeo-
Productivity
Preservation
Open/
Upwelling
Restricted
Cd/ Mo
Co [mg/kg] x Mn [%]
b
Deepwater age or renewal time (yrs)
Sediment Mo/TOC
Saanich Inlet
Framvaren Fjord
Cariaco Basin
Black Sea
Lower
Posidonia Shale
Upper
Posidonia Shale
Lower
Posidonia Shale
Reduced global seawater
Mo inventory?
?
Hebrides Basin
Lusitanian Basin
Cleveland Basin & West Netherlands Basin
Paris Basin
South German Basin
Dutch Central Grabem
Asturian Basin
Belluno Basin
Atlassic Basin

◂**Fig. 8** **a** Cd/Mo versus Co*Mn concentrations and **b** Mo/TOC ratios of Posidonia Shale sediments in Core A (Dickson et al. 2022), compared to sedimentary values in present-day and Toarcian anoxic–euxinic depositional environments and to modern deepwater renewal times (Algeo and Lyons 2006; Fernandez-Martínez et al. 2023)

domain, the First Occurrence of *C. superbus* occurs in few cases at the base or within the *H. serpentinum* (equivalent to *H. falciferum*) ammonite Zone (e.g., the Schandelah core in North Germany; van de Schootbrugge et al. 2019). However, the diachroneity in the FO of *C. superbus* is only apparent and likely due to discrepancies in the sample density or in the ammonite record. In fact, in some localities the ammonite record is very scarce in the organic-rich interval. Alternatively, the occurrence of condensed levels or hiatuses in the lower Toarcian of many Tethyan sections may also account for some differences in terms of ranking of nannofossil bioevents, as discussed by Menini et al. (2018).

Carbon-isotope values remain relatively stable following the overall $\delta^{13}C_{TOC}$ positive excursion, similar to the trend observed in the Mochras core (Xu et al. 2018a), up to the top of the Posidonia Shale Formation and covering the NJT6 and NJT7 nannofossil zones. Bio- and chemostratigraphic correlation to the Mochras core suggests that the top of the preserved Posidonia Shale succession in the LSB correlates to a *H. bifrons* or *H. variabilis* biozone age (Fig. 7). Such an age is consistent with the one provided by nannofossil data. In fact, the NJT8 Zone correlates to the *H. (B). gradata* (*H. variabilis*) ammonite Zone (Ferreira et al. 2019). At Dotternhausen, the Posidonia Shale also corresponds to the *C. superbus* (NJT6) and the *D. striatus* (NJT7) nannofossil biozones; however, the Posidonia Shale is much thinner there (~4.5 m of 'Oil Shale', overlain by ~5.5 m of 'Bituminous Mudstone' at Dotternhausen (Schmid-Röhl et al. 2002), compared to ~35 m in Core A.

The top of the Posidonia Shale in the LSB is characterized by a 2‰ positive shift in carbon-isotope values, condensed sediment, with abundant micro-bored belemnite debris and a hiatus (Hiatus D), with calcareous nannofossils assigning the strata of the overlying Jurensismergel to the *R. incompta* Zone (NJT8a) of middle to late(?) Toarcian age.

Reduced sediment supply and erosion during the T-OAE in the Lower Saxony Basin

The Posidonia Shale is commonly considered to have formed coevally with the T-OAE and associated negative CIE in the Germanic basins, with an observed ~4 m thick negative CIE in ~14 m thick Posidonia Shale successions in locations in SW Germany (Rohl et al. 2001; Schmid-Röhl et al. 2002; Schwark and Frimmel 2004). In the Lower Saxony Basin, however, the T-OAE negative CIE interval (including hiatuses) is stratigraphically restricted to the lower ~3 m of the Posidonia Shale Formation, which is on average ~35 m thick. This stratigraphy suggests that early Toarcian sedimentation rates in the SW Germanic basins were significantly reduced because of either limited accommodation space or sediment starvation, or both, whereas higher subsidence rates likely caused the deposition of a much thicker, and possibly more complete (bar the hiatus-riddled T-OAE interval) Posidonia Shale in the Lower Saxony Basin.

The onset of the T-OAE is commonly associated with the development of condensed sedimentation and/or the occurrence of stratigraphic gaps in geographically widespread sedimentary deposits such as the Neuquén Basin in Argentina (Al-Suwaidi et al. 2010, 2016), sections in France, Spain, Portugal, and the UK (Hesselbo and Jenkyns 1998; Gómez et al. 2008; Hesselbo 2008; Mailliot et al. 2009; Kemp et al. 2011; Sandoval et al. 2012; Suan et al. 2015; Martinez et al. 2017; Bodin et al. 2023), western Canada (Caruthers et al. 2011), as well as in northern Siberia (Suan et al. 2011; Ruebsam et al. 2020). The globally recognized condensed nature of sedimentation at the base of the T-OAE interval has been interpreted as a consequence of eustatic sea-level rise leading to sediment starvation in some basins (Hallam 1997; Al-Suwaidi et al. 2010; Pittet et al. 2014; Montero-Serrano et al. 2015; Thibault et al. 2018). However, such an interpretation may be complicated by local Early Jurassic tectonism. Short-term relative sea-level changes around Pliensbachian–Toarcian boundary time occurred superimposed on a late Pliensbachian sea-level low-stand that preceded major sea-level rise during the early Toarcian (e.g., Hallam 1997; Hesselbo and Jenkyns 1998; Hesselbo 2008; Haq 2017; Bodin et al. 2023). This inferred widespread, potentially largely global, sea-level evolution is corroborated by carbonate platforms showing initial subaerial exposure followed by early Toarcian drowning (Blomeier and Reijmer 1999; Woodfine et al. 2008; Léonide et al. 2012; Sandoval et al. 2012).

The Lower Saxony Basin sedimentary record suggests long-term relative sea-level rise from the depositional interval of the Amaltheenton Formation to the Posidonia Shale, with decreasing grain-size and the loss of thin turbiditic horizons and shell debris, as well as the more consistent occurrence of calcareous nannofossils. However, superimposed on the longer-term sedimentary evolution, inferred Hiatus A (at 45 m) and Hiatus B (43.5 m) suggest sediment winnowing, potentially from rapid relative sea-level fall during the earliest Toarcian and associated erosion or non-deposition, possibly modulated by irregular basin morphology and local bathymetric highs, causing the T-OAE to have only been partially recorded in the Lower Saxony Basin. However, the origin of hiatuses in mudstone is a long-standing point of debate going back for example to Fürsich

et al. (1992), Hallam (1999), Wetzel and Allia (2000),and Coe and Hesselbo (2000); condensation and erosion could, in principle, result from either sediment starvation due to sea-level rise, or increased energy on the seafloor due to sea-level fall, and it is often difficult to tell the causes apart.

Erosional and condensed horizons for a similar stratigraphic interval were also reported for the Schandelah core from northern Germany (van de Schootbrugge et al. 2019), as well as in basins further afield (Ruebsam et al. 2020), supporting the role of eustatic sea-level changes in controlling the local depositional environment. Subsequent relative sea-level rise at the onset of the T-OAE then led to the development of deeper water conditions. Combined, our data suggest that eustatic sea-level change, as well as local bathymetric conditions, played an important role in controlling sediment supply, deposition and erosion, particularly around the Pliensbachian–Toarcian transition and during the early Toarcian in the LSB, as recorded in Core A. In addition, global climatic and environmental forcing associated with the T-OAE controlled water-column chemistry (Dickson et al. 2017, 2022) and the deposition of the characteristic organic-rich black shales of the Posidonia Shale.

Prolonged basin restriction and water-column anoxia as the cause for protracted Toarcian organic-matter burial in the Lower Saxony Basin

Deposition of the Posidonia Shale in the Lower Saxony Basin continued significantly after the T-OAE negative CIE, which suggests a prolonged period of perturbed environmental conditions promoted the deposition of organic-rich black shale long after the organic-rich sediment formation had ceased in other basins across the NW European seaway. High sedimentary TOC values through the T-OAE interval are commonly linked to elevated organic primary productivity in the surface waters inducing water-column anoxia–euxinia, and enhancing sedimentary organic matter preservation with, in addition, possibly reduced sedimentation rates (Kemp et al. 2022a, b; Ruebsam and Schwark 2024). Redox- and productivity-sensitive trace and major elemental concentrations (Co*Mn) and ratios (Cd/Mo) are commonly used to infer palaeo water-column redox states (Sweere et al. 2016; McArthur 2019). Utilizing available data from the Posidonia Shale in the studied core of the Lower Saxony Basin it appears that Toarcian organic-carbon burial here was largely driven by elevated preservation, under conditions of basin restriction (marked by water-column stratification, anoxia and elevated carbon burial fluxes) that were extreme relative to such modern-day settings (Fig. 8) (Algeo and Lyons 2006; Sweere et al. 2016; Dickson et al. 2022). The observed sedimentary molybdenum-isotope and Mo/TOC values in the wider Germanic Basin (Dickson et al. 2017) and the core studied here, respectively, suggest that the lower part of the Posidonia Shale in the Lower Saxony Basin formed under anoxic–euxinic conditions with a relatively long (10^2–10^3 years) deep-water age or renewal time (Algeo and Lyons 2006; Dickson et al. 2022). Observed sedimentary Mo/TOC values for the upper part of the Posidonia Shale suggest an even more restricted environment, similar to the present-day Black Sea (Algeo and Lyons 2006; Dickson et al. 2022), in line with observed Mo/TOC values for lower Toarcian black shales in adjacent basins across the north European seaway (Thibault et al. 2018; Remirez and Algeo 2020a and b; Fernandez-Martínez et al. 2023). Importantly, the thermally early mature nature of the Posidonia Shale in core A may have enhanced the Mo/TOC ratio (Lewan et al. 1983; Dickson et al. 2020); therefore, the basinal deep-water age or renewal times suggested by the Mo/TOC values of the here studied Posidonia Shale sediments, and in comparison to modern-day marine sediment values, may in actuality have been longer. However, the global ocean Mo inventory (and by inference water-column Mo concentrations) were likely significantly lower during (parts of) the early Toarcian, impacting on the interpreted water-column renewal times for individual basins.

The overall Lower Saxony Basin history and persistence of anoxic conditions well after the T-OAE negative CIE was not limited to this basin alone, nor even the European epicontinental seaway, but has also been reported from, for example, the Cleveland Basin (U.K., e.g., Atkinson et al. 2023), the Western Canada Sedimentary Basin (Them et al. 2018) and, to some extent, the Paris Basin (van Breugel et al. 2006; Hermoso et al. 2013).

Conclusions

High-resolution carbon-isotope stratigraphy combined with calcareous nannofossil biostratigraphy in Core A of the Lower Saxony Basin (LSB), Germany, constrains deposition of the studied sedimentary succession to the Lower Jurassic Pliensbachian and Toarcian stages. The upper Pliensbachian Amaltheenton Formation and Toarcian Posidonia Shale Formation in the Lower Saxony Basin record the Pliensbachian–Toarcian boundary event as well as the Toarcian oceanic anoxic event (T-OAE), and the associated carbon-isotope excursions (CIEs). Similarly to other sections in NW Europe, the onset of the T-OAE interval was characterized by condensed sedimentation and hiatuses, possibly because of a sea-level low-stand during the latest Pliensbachian and earliest Toarcian. The T-OAE negative CIE in core A of the LSB, albeit interrupted by hiatuses, is recorded over a 3-m stratigraphical interval at the base of the Posidonia Shale, with TOC values between 1% and 14%. This interval is stratigraphically followed by another ~27 m of organic-rich black shales of the Posidonia Shale Formation, with TOC

values of on average ~10% (varying between 4% and 14.5%), that were laid down stratigraphically following the T-OAE. The observed pattern of sedimentation suggests protracted local perturbance of the basinal depositional environment, with hydrographic restriction and likely longer basin-water renewal times having contributed to continued, relatively elevated carbon burial in the Lower Saxony Basin, setting it apart from adjacent basins across the north European sectors of the Laurasian seaway.

Supplementary Information The online version contains supplementary material available at https://doi.org/10.1007/s00531-024-02477-9.

Acknowledgements This study was funded by Shell Global Solutions International B.V. ExxonMobil Production Deutschland GmbH provided access to core materials. RS was funded by the University of Exeter as part of the NERC Oil and Gas Doctoral Training College. We thank Mrs Ghislaine Broillet for preparation of smear slides for calcareous nannofossil analyses. We sincerely thank the guest-editor of this Special Issue, Christoph Hartkopf-Fröder, reviewer Mariano Remirez, and one anonymous reviewer for their thorough and constructive comments and suggestions, which significantly improved this manuscript. This is a contribution to UNESCO IGCP Project 739—The Mesozoic and Palaeogene Hyperthermal Events.

Funding This study was funded by Shell Global Solutions International B.V.

Data availability All here published data are available in the Online Supplementary Information files provided with this paper.

References

Algeo TJ, Lyons TW (2006) Mo-total organic carbon covariation in modern anoxic marine environments: Implications for analysis of paleoredox and paleohydrographic conditions. Paleoceanography 21:PA1016. https://doi.org/10.1029/2004PA001112

Al-Suwaidi AH, Angelozzi GN, Baudin F, Damborenea SE, Hesselbo SP, Jenkyns HC, Mancenido MO, Riccardi AC (2010) First record of the early Toarcian Oceanic Anoxic Event from the Southern Hemisphere, Neuquén Basin, Argentina. J Geol Soc 167:633–636

Al-Suwaidi AH, Hesselbo SP, Damborenea SE, Manceñido MO, Jenkyns HC, Riccardi AC, Angelozzi GN, Baudin F (2016) The Toarcian Oceanic Anoxic Event (Early Jurassic) in the Neuquén Basin, Argentina: a reassessment of age and carbon Iisotope stratigraphy. J Geol 124(2):171–193

Al-Suwaidi AH, Ruhl M, Jenkyns HC, Damborenea SE, Manceñido MO, Condon DJ, Angelozzi GN, Kamo SL, Storm M, Riccardi AC, Hesselbo SP (2022) New age constraints on the Lower Jurassic Pliensbachian–Toarcian Boundary at Chacay Melehue (Neuquén Basin, Argentina). Sci Rep 12:4975

Atkinson JW, Little CTS, Dunhill AM (2023) Long duration of benthic ecological recovery from the early Toarcian (Lower Jurassic) mass extinction event in the Cleveland Basin, UK. J Geol Soc Lond 180(2):jgs2022–jgs2126

Baghli H, Mattioli E, Spangenberg JE, Bensalah M, Arnaud-Godet F, Pittet B, Suan G (2020) Early Jurassic climatic trends in the south-Tethyan margin. Gondwana Res 77:67–81

Bailey TR, Rosenthal Y, McArthur JM, van de Schootbrugge B, Thirlwall MF (2003) Paleoceanographic changes of the Late Pliensbachian – early Toarcian interval: a possible link to the genesis of an Oceanic Anoxic Event. Earth Planet Sci Lett 212:307–320

Behar F, Beaumont VDEB, Penteado HDB (2001) Rock-Eval 6 technology: performances and developments. Oil Gas Sci Technol 56:111–134

Betz D, Führer F, Greiner G, Plein E (1987) Evolution of the Lower Saxony Basin. Tectonophysics 137:127–170

Blomeier DPG, Reijmer JJG (1999) Drowning of a Lower Jurassic carbonate platform: Jbel Bou Dahar, High Atlas, Morocco. Geobios 41:81–10

Bodin S, Krencker FN, Kothe T, Hoffmann R, Mattioli E, Heimhofer U, Kabiri L (2016) Perturbation of the carbon cycle during the late Pliensbachian - early Toarcian: new insight from high-resolution carbon isotope records in Morocco. J Afr Earth Sci 116:89–104

Bodin S, Fantasia A, Krencker FN, Nebsbjerg B, Christiansen L, Andrieu S (2023) More gaps than record! A new look at the Pliensbachian/Toarcian boundary event guided by coupled chemo-sequence stratigraphy. Palaeogeogr Palaeoclimatol Palaeoecol 610:111344

Bown PR, Cooper MKE (1998) Jurassic. In: Bown PR (ed) Calcareous nannofossil biostratigraphy, british micropalaeontological society publication series. Kluwer Academic Publishers, Dordrecht-Boston-London, pp 34–54

Bown PR, Young JR (1998) Introduction. In: Bown PR (ed) Calcareous nannofossil biostratigraphy, british micropalaeontological society publication series. Kluwer Academic Publishers, Dordrecht-Boston-London, pp 1–15

Brink HJ, Dürschner H, Trappe H (1992) Some aspects of the late and post-Variscan development of the Northwestern German Basin. Tectonophysics 207:65–95

Bruns B, di Primio R, Berner U, Littke R (2013) Petroleum system evolution in the inverted Lower Saxony Basin, northwest Germany: a 3D basin modeling study. Geofluids 13:246–271

Bucefalo Palliani RB, Mattioli E (1998) High resolution integrated microbiostratigraphy of the Lower Jurassic (late Pliensbachian-early Toarcian) of central Italy. J Micropalaeontol 17:153–172

Caruthers AH, Gröcke DR, Smith PL (2011) The significance of an Early Jurassic (Toarcian) carbon-isotope excursion in Haida Gwaii (Queen Charlotte Islands), British Columbia, Canada. Earth Planet Sci Lett 307:19–26

Caswell BA, Coe AL (2014) The impact of anoxia on pelagic macrofauna during the Toarcian Oceanic Anoxic Event (Early Jurassic). Proc Geol Assoc 125:383–391

Coe AL, Hesselbo SP (2000) Discussion of Hallam (1999). "Evidence of sea-level fall in sequence stratigraphy: examples from the Jurassic." Geology 28:95

Cohen AS, Coe AL, Harding SM, Schwark L (2004) Osmium isotope evidence for the regulation of atmospheric CO_2 by continental weathering. Geology 32:157–160

Copestake P, Johnson B (2013) Lower Jurassic foraminifera from the Llanbedr (Mochras Farm) borehole, North Wales, UK. Monogr Palaeontol Soc Lond 167(641):1–403

da Rocha RB, Mattioli E, Duarte LV, Pittet B, Elmi S, Mouterde R, Cabral MC, Comas-Rengifo MJ, Gomez JJ, Goy A, Hesselbo SP, Jenkyns HC, Littler K, Mailliot S, Veiga de Oliveira LC, Osete ML, Perili N, Pinto S, Ruget C, Suan G (2016) Base of the Toarcian Stage of the Lower Jurassic defined by the Global Boundary Stratotype Section and Point (GSSP) at the Peniche section (Portugal). Episodes 39(3):460–481

De Lena LF, Taylor D, Guex J, Bartolini A, Adatte T, van Acken D, Spangenberg JE, Samankassou E, Vennemann T, Schaltegger U (2019) The driving mechanisms of the carbon cycle perturbations in the late Pliensbachian (Early Jurassic). Sci Rep 9:18430. https://doi.org/10.1038/s41598-019-54593-1

Dickson AJ, Gill BC, Ruhl M, Jenkyns HC, Porcelli D, Idiz E, Lyons TW, van den Boorn SHJM (2017) Molybdenum-isotope chemostratigraphy and paleoceanography of the Toarcian Oceanic Anoxic Event (Early Jurassic). Paleoceanography 32:813–829

Dickson AJ, Idiz E, Porcelli D, van den Boorn SHJM (2020) The influence of thermal maturity on the stable isotope compositions and concentrations of molybdenum, zinc and cadmium in organic-rich marine mudrocks. Geochim Cosmochim Acta 287:205–220

Dickson AJ, Idiz E, Porcelli D, Murphy MJ, Celestino R, Jenkyns HC, Poulton SW, Hesselbo SP, Hooker JN, Ruhl M, van den Boorn SHJM (2022) No effect of thermal maturity on the Mo, U, Cd, and Zn isotope compositions of Lower Jurassic organic-rich sediments. Geology 50:598–602

Erba E, Cavalheiro L, Dickson AJ, Faucher G, Gambacorta G, Jenkyns HC, Thomas W (2022) Carbon and oxygen-isotope signature of the Toarcian Oceanic Anoxic Event: insights from two Tethyan pelagic sequences (Gajum and Sogno Cores, Lombardy Basin, northern Italy). Newsl Stratigr 55:451–477

Fantasia A, Föllmi KB, Adatte T, Bernárdez E, Spangenberg JE, Mattioli E (2018) The Toarcian oceanic anoxic event in southwestern Gondwana: an example from the Andean Basin, northern Chile. J Geol Soc 175:883–902

Fantasia A, Adatte T, Spangenberg JE, Font E, Duarte LV, Föllmi KB (2019) Global versus local processes during the Pliensbachian-Toarcian transition at the Peniche GSSP, Portugal: a multi-proxy record. Earth Sci Rev 198:102932

Fernandez-Martínez J, Martinez Ruiz F, Rodriguez-Tovar FJ, Pinuela L, Garcia-Ramos JC, Algeo TJ (2023) Euxinia and hydrographic restriction in the Tethys Ocean: reassessing global oceanic anoxia during the early Toarcian. Global Planet Change 221:104026

Ferreira J, Mattioli E, Sucheras-Marx B, Giraud F, Duarte LV, Pittet B, Suan G, Hassler A, Spangenberg JE (2019) Western Tethys Early and Middle Jurassic calcareous nannofossil biostratigraphy. Earth Sci Rev 197:102908

Fraguas Á, Comas-Rengifo MJ, Perilli N (2015) Calcareous nannofossil biostratigraphy of the Lower Jurassic in the Cantabrian Range (Northern Spain). Newsl Stratigr 48:179–199

Frimmel A, Oschmann W, Schwark L (2004) Chemostratigraphy of the Posidonia Black Shale, SW Germany I. Influence of sea-level variation on organic facies evolution. Chem Geol 206:199–230

Fürsich FT, Oschmann W, Singh IB, Jaitly AK (1992) Hardgrounds, reworked concretion levels and condensed horizons in the Jurassic of western India: their significance for basin analysis. J Geol Soc 149:313–331

Gambacorta G, Brumsack HJ, Jenkyns HC, Erba E (2024) The early Toarcian Oceanic Anoxic Event (Jenkyns Event) in the Alpine-Mediterranean Tethys, north African margin, and north European epicontinental seaway. Earth Sci Rev 248:104636

Gómez JJ, Goy A, Canales ML (2008) Seawater temperature and carbon isotope variations in belemnites linked to mass extinction during the Toarcian (Early Jurassic) in Central and Northern Spain. Comparison with other European sections. Palaeogeogr Palaeoclimatol Palaeoecol 258:28–58

Gorbanenko OO (2015) High-resolution organic petrography of the Toarcian Posidonia Shale of Germany and the western Netherlands: study of the organo-mineral microfacies variations, reconstruction of the depositional environments and construction of a depositional model. Ph.D. thesis, University of Tübingen

Gorbanenko OO, Ligouis B (2014) Changes in optical properties of liptinite macerals from early mature to post mature stage in Posidonia Shale (lower Toarcian, NW Germany). Int J Coal Geol 133:47–59

Hallam A (1997) Estimates of the amount and rate of sea-level change across the Rhaetian-Hettangian and Pliensbachian-Toarcian boundaries (latest Triassic to early Jurassic). J Geol Soc 154:773–779

Hallam A (1999) Evidence of sea-level fall in sequence stratigraphy: examples from the Jurassic. Geology 27:333–346

Harries PJ, Little CT (1999) The early Toarcian (Early Jurassic) and the Cenomanian-Turonian (Late Cretaceous) mass extinctions: Similarities and contrasts. Palaeogeogr Palaeoclimatol Palaeoecol 154:39–66

Haq BU (2017) Jurassic Sea-Level Variations: A Reappraisal. GSA Today 28(1). https://doi.org/10.1130/GSATG359A

Heimdal TH, Goddéris Y, Jones MT, Svensen HH (2021) Assessing the importance of thermogenic degassing from the Karoo Large Igneous Province (LIP) in driving Toarcian carbon cycle perturbations. Nat Commun 12:6221

Hermoso M, Le Callonnec L, Minoletti F, Renard M, Hesselbo SP (2009) Expression of the early Toarcian negative carbon-isotope excursion in separated carbonate microfractions (Jurassic, Paris Basin). Earth Planet Sci Lett 277:194–203

Hermoso M, Minoletti F, Pellenard P (2013) Black shale deposition during Toarcian super-greenhouse driven by sea level. Clim past 9:2703–2712

Hesselbo SP (2008) Sequence stratigraphy and inferred relative sea-level change from the onshore British Jurassic. Proc Geol Assoc 119(1):19–34

Hesselbo SP, Jenkyns HC (1998) British Lower Jurassic sequence stratigraphy. In: de Graciansky PC, Hardenbol J, Jacquin T, Farley M, Vail, PR (eds) Mesozoic–Cenozoic Sequence Stratigraphy of European Basins. Special Publication of the Society for Sedimentary Geology (SEPM), pp 60:561–581.

Hesselbo SP, Palmer TJ (1992) Reworked early diagenetic concretions and the bioerosional origin of a regional discontinuity within British Jurassic marine mudstones. Sedimentology 39:1045–1065

Hesselbo SP, Pienkowski G (2011) Stepwise atmospheric carbon isotope excursion during the Toarcian Oceanic Anoxic Event (Early Jurassic, Polish Basin). Earth Planet Sci Lett 301:365–372

Hesselbo SP, Gröcke DR, Jenkyns HC, Bjerrum CJ, Farrimond P, Morgans Bell HS, Green OR (2000) Massive dissociation of gas hydrate during a Jurassic oceanic anoxic event. Nature 406:392–395

Hesselbo SP, Robinson SA, Surlyk F (2004) Sea-level change and facies development across potential Triassic-Jurassic boundary horizons, SW Britain. J Geol Soc 161:365–379

Hesselbo SP, Jenkyns HC, Duarte LV, Oliveira LCV (2007) Carbon-isotope record of the Early Jurassic (Toarcian) Oceanic Anoxic Event from fossil wood and marine carbonate (Lusitanian Basin, Portugal). Earth Planet Sci Lett 253:455–470

Hooker JN, Ruhl M, Dickson AJ, Hansen LN, Idiz E, Hesselbo SP, Cartwright J (2020) Shale anisotropy and natural hydraulic fracture propagation: an example from the

Jurassic (Toarcian) Posidonienschiefer, Germany. JGR Solid Earth 125(3):e2019JB018442
Ikeda M, Hori RS (2014) Effects of Karoo-Ferrar volcanism and astronomical cycles on the Toarcian oceanic anoxic events (Early Jurassic). Palaeogeogr Palaeoclimatol Palaeoecol 410:134–142
Ivimey-Cook HC (1971) Stratigraphical palaeontology of the Lower Jurassic of the Llanbedr (Mochras Farm) Borehole. In: The Llanbedr (Mochras Farm) Borehole (Ed. by A. W. Woodland), Report Inst. Geol. Sci. 71(18): 87–92.
Jenkyns HC (1985) The early Toarcian and Cenomanian-Turonian anoxic events in Europe: comparisons and contrasts. Geol Rundsch 74:505–518
Jenkyns HC (1988) The early Toarcian (Jurassic) anoxic event: stratigraphic, sedimentary, and geochemical evidence. Am J Sci 288:101–151
Jenkyns HC (2010) Geochemistry of oceanic anoxic events. Geochem Geophys Geosyst 11:Q03004. https://doi.org/10.1029/2009GC002788
Jenkyns HC, Clayton CJ (1987) Lower Jurassic epicontinental carbonates and mudstones from England and Wales: chemostratigraphic signals and the early Toarcian anoxic event. Sedimentology 44:687–706
Jenkyns HC, Jones CE, Gröcke DR, Hesselbo SP, Parkinson DN (2002) Chemostratigraphy of the Jurassic System: applications, limitations and implications for palaeoceanography. J Geol Soc 159:351–378
Jones MT, Jerram DA, Svensen HH, Grove C (2016) The effects of large igneous provinces on the global carbon and sulphur cycles. Palaeogeogr Palaeoclimatol Palaeoecol 441:4–21
Kafousia N, Karakitsios V, Jenkyns HC, Mattioli E (2011) A global event with a regional character: the Early Toarcian Oceanic Anoxic Event in the Pindos Ocean (northern Peloponnese, Greece). Geol Mag 148:619–631
Kemp DB, Izumi K (2014) Multiproxy geochemical analysis of a Panthalassic margin record of the early Toarcian oceanic anoxic event (Toyora area, Japan). Palaeogeogr Palaeoclimatol Palaeoecol 414:332–341
Kemp DB, Coe AL, Cohen AS, Schwark L (2005) Astronomical pacing of methane release in the Early Jurassic period. Nature 437:396–399
Kemp DB, Coe AL, Cohen AS, Weedon GP (2011) Astronomical forcing and chronology of the early Toarcian (Early Jurassic) oceanic anoxic event in Yorkshire, UK. Paleoceanography. https://doi.org/10.1029/2011PA002122
Kemp DB, Chen W, Cho T, Algeo TJ, Shen J, Ikeda M (2022a) Deep-ocean anoxia across the Pliensbachian-Toarcian boundary and the Toarcian Oceanic Anoxic Event in the Panthalassic Ocean. Global Planet Change 212:103782
Kemp DB, Suan G, Fantasia A, Jin S, Chen W (2022b) Global organic carbon burial during the Toarcian oceanic anoxic event: Patterns and controls. Earth Sci Rev 231:104086
Korte C, Hesselbo SP, Ullmann CV, Dietl G, Ruhl M, Schweigert G, Thibault N (2015) Jurassic climate mode governed by ocean gateway. Nat Commun 6:10015
Küspert W (1982) Environmental changes during oil shale deposition as deduced from stable isotope ratios. In: Einsele G, Seilacher A (eds) Cyclic and event stratification. Springer, Berlin-Heidelberg, pp 482–501
Léonide P, Floquet M, Durlet C, Baudin F, Pittet B, Lécuyer C (2012) Drowning of a carbonate platform as a precursor stage of the early Toarcian global anoxic event (Southern Provence sub-Basin, South-East France). Sedimentology 59:156–184
Lewan MD (1983) Effects of thermal maturation on stable organic carbon isotopes as determined by hydrous pyrolysis of Woodford Shale. Geochim Cosmochim Acta 47:1471–1479
Littke R, Leythaeuser D, Rullkötter J, Baker DR (1991) Keys to the depositional history of the Posidonia Shale (Toarcian) in the Hils Syncline, northern Germany. Geol Soc Lon Spec Pub 58:311–333
Littler K, Hesselbo SP, Jenkyns HC (2010) A carbon-isotope perturbation at the Pliensbachian-Toarcian boundary: evidence from the Lias Group, NE England. Geol Mag 147:181–192
Mailliot S, Mattioli E, Bartolini A, Baudin F, Pittet B, Guex J (2009) Late Pliensbachian-early Toarcian (Early Jurassic) environmental changes in an epicontinental basin of NW Europe (Causses area, central France): a micropaleontological and geochemical approach. Palaeogeogr Palaeoclimatol Palaeoecol 273:346–364
Marten T, Ruebsam W, Mutterlose JB, Wiesenberg GLB, Schwark L (2024) Latest Pliensbachian to early Toarcian depositional environment and organo-facies evolution in the North-German Basin (Hondelage Section). Int J Earth Sci (Geologische Rundschau). https://doi.org/10.1007/s00531-024-02433-7
Martinez M, Krencker FN, Mattioli E, Bodin S (2017) Orbital chronology of the Pliensbachian-Toarcian transition from the Central High Atlas Basin (Morocco). Newsl Stratigr 50:47–69
Mattioli E, Erba E (1999) Synthesis of calcareous nannofossil events in Tethyan Lower and Middle Jurassic successions. Riv Ital Paleontol Stratigr 105:343–376
Mattioli E, Pittet B, Bucefalo Palliani R, Röhl H-J, Schmid-Röhl A, Morettini E (2004) Phytoplankton evidence for the timing and correlation of palaeoceanographical changes during the early Toarcian oceanic anoxic event (Early Jurassic). J Geol Soc 161:685–693
Mattioli E, Pittet B, Suan G, Mailliot S (2008) Calcareous nannoplankton changes across the early Toarcian oceanic anoxic event in the western Tethys. Paleoceanography 23:PA3208
Mattioli E, Pittet B, Petitpierre L, Mailliot S (2009) Dramatic decrease of the pelagic carbonate production by nannoplankton across the early Toarcian Anoxic Event (T-OAE). Global Planet Changes 65:134–145. https://doi.org/10.1016/j.gloplacha.2008.10.018
Mattioli E, Plancq J, Boussaha M, Duarte LV, Pittet B (2013) Calcareous nannofossil biostratigraphy: new data from the Lower Jurassic of the Lusitanian Basin. Comunicações Geológicas 100:69–76
McArthur JM (2019) early Toarcian black shales: a response to an oceanic anoxic event or anoxia in marginal basins? Chem Geol 522:71–83
McArthur JM, Donovan DT, Thirlwall MF, Fouke BW, Mattey D (2000) Strontium isotope profile of the early Toarcian (Jurassic) oceanic anoxic event, the duration of ammonite biozones, and belemnite palaeotemperatures. Earth Planet Sci Lett 179:269–285
McCann T (2008) The geology of Central Europe (Volume 2): Mesozoic and Cenozoic. The Geological Society, London
McElwain JC, Wade-Murphy J, Hesselbo SP (2005) Changes in carbon dioxide during an oceanic anoxic event linked to intrusion into Gondwana coals. Nature 435:479–482
Menini A, Mattioli E, Spangenberg JE, Pittet B, Suan G (2018) New calcareous nannofossil and carbon isotope data for the Pliensbachian/Toarcian boundary (Early Jurassic) in the western Tethys and their paleoenvironmental implications. Newsl Stratigr 52:173–196
Menini A, Mattioli E, Hesselbo SP, Ruhl M, Suan G (2021) Primary v. carbonate production in the Toarcian, a case study from the Llanbedr (Mochras Farm) borehole, Wales. Geol Soc Lond Spec Publ 514(1):59

Montero-Serrano J-C, Föllmi KB, Adatte T, Spangenberg JE, Tribovillard N, Fantasia A, Suan G (2015) Continental weathering and redox conditions during the early Toarcian Oceanic Anoxic Event in the northwestern Tethys: insight from the Posidonia Shale section in the Swiss Jura Mountains. Palaeogeogr Palaeoclimatol Palaeoecol 429:83–99

Percival LM, Witt ML, Mather TA, Hermoso M, Jenkyns HC, Hesselbo SP, Al-Suwaidi AH, Storm MS, Xu W, Ruhl M (2015) Globally enhanced mercury deposition during the end-Pliensbachian extinction and Toarcian OAE: a link to the Karoo-Ferrar Large Igneous Province. Earth Planet Sci Lett 428:267–280

Percival LME, Cohen AS, Davies MK, Dickson AJ, Hesselbo SP, Jenkyns HC, Leng MJ, Mather TA, Storm MS, Xu W (2016) Osmium isotope evidence for two pulses of increased continental weathering linked to Early Jurassic volcanism and climate change. Geology 44(9):759–762

Peti L, Thibault N, Clémence ME, Korte C, Dommergues JL, Bougeault C, Pellenard P, Jelby ME, Ullmann CV (2017) Sinemurian-Pliensbachian calcareous nannofossil biostratigraphy and organic carbon isotope stratigraphy in the Paris Basin: Calibration to the ammonite biozonation of NW Europe. Palaeogeogr Palaeoclimatol Palaeoecol 468:142–161

Pieńkowski G, Uchman A, Ninard K, Page KN, Hesselbo SP (2024) Early Jurassic extrinsic solar system dynamics versus intrinsic Earth processes – Toarcian sedimentation and benthic life in deep-sea contourite drift facies, Cardigan Bay Basin, UK. Progress Earth Planet Sci 11:18

Pittet B, Suan G, Lenoir F, Duarte LV, Mattioli E (2014) Carbon isotope evidence for sedimentary discontinuities in the lower Toarcian of the Lusitanian Basin (Portugal): sea level change at the onset of the Oceanic Anoxic Event. Sed Geol 303:1–14

Remírez MN, Algeo TJ (2020a) Carbon-cycle changes during the Toarcian (Early Jurassic) and implications for regional versus global drivers of the Toarcian oceanic anoxic event. Earth Sci Rev 209:103283

Remírez MN, Algeo TJ (2020b) Paleosalinity determination in ancient epicontinental seas: a case study of the T-OAE in the Cleveland Basin (UK). Earth Sci Rev 201:103072

Riegraf W, Werner G, Lörcher F (1984) Der Posidonienschiefer: Biostratigraphie, Fauna und Fazies des südwestdeutschen Untertoarciums (Lias ε): F. Enke, Stuttgart

Röhl HJ, Schmid-Röhl A, Oschmann W, Frimmel A, Schwark L (2001) The Posidonia Shale (lower Toarcian) of SW Germany: an oxygen depleted ecosystem controlled by sea level and paleoclimate. Palaeogeogr Palaeoclimatol Palaeoecol 165:27–52

Roth PH (1984) Preservation of calcareous nannofossils and fine-grained carbonate particles in mid-Cretaceous sediments from the southern Angola Basin, Site 530. In: Hay WW (ed) Initial reports of deep sea drilling project 75. Government Printing Office, Washington, U.S, pp 651–655

Ruebsam W, Schwark L (2024) Disparity between Toarcian Oceanic Anoxic Event and Toarcian carbon isotope excursion. Int J Earth Sci. https://doi.org/10.1007/s00531-024-02408-8

Ruebsam W, Müller T, Kovács J, Pálfy J, Schwark L (2018) Environmental response to the early Toarcian carbon cycle and climate perturbations in the northeastern part of the West Tethys shelf. Gondwana Res 59:144–158

Ruebsam W, Reolid M, Sabatino N, Masetti D, Schwark L (2020) Molecular paleothermometry of the early Toarcian climate perturbation. Global Planet Change 195:103351

Ruhl M, Hesselbo SP, Jenkyns HC, Xu W, Silva RL, Matthews KJ, Mather TA, Mac Niocaill C, Riding JB (2022) Reduced plate motion controlled timing of Early Jurassic Karoo-Ferrar large igneous province volcanism. Sci Adv 8:eabo0866

Sabatino N, Neri R, Bellanca A, Jenkyns HC, Baudin F, Parisi G, Masetti D (2009) Carbon-isotope records of the Early Jurassic (Toarcian) oceanic anoxic event from the Valdorbia (Umbria-Marche Apennines) and Monte Mangart (Julian Alps) sections: palaeoceanographic and stratigraphic implications. Sedimentology 56:1307–1328

Sabatino N, Vlahović I, Jenkyns HC, Scopelliti G, Neri R, Prtoljan B, Velić I (2013) Carbon-isotope record and palaeoenvironmental changes during the early Toarcian oceanic anoxic event in shallow-marine carbonates of the Adriatic Carbonate Platform in Croatia. Geol Mag 150:1085–1102

Sandoval J, Bill M, Aguado R, O'Dogherty L, Rivas P, Morard A, Guex J (2012) The Toarcian in the Subbetic basin (southern Spain): Bioevents (ammonite and calcareous nannofossils) and carbon-isotope stratigraphy. Palaeogeogr Palaeoclimatol Palaeoecol 342–343:40–63

Schmid-Röhl A, Röhl HJ (2003) Overgrowth on ammonite conchs: environmental implications for the lower Toarcian Posidonia Shale. Palaeontology 46:339–352

Schmid-Röhl A, Röhl HJ, Oschmann W, Frimmel A, Schwark L (2002) Palaeoenvironmental reconstruction of lower Toarcian epicontinental black shales (Posidonia Shale, SW Germany): global versus regional control. Geobios 35:13–20

Schwark L, Frimmel A (2004) Chemostratigraphy of the Posidonia Black Shale, SW-Germany II. Assessment of extent and persistence of photic-zone anoxia using aryl isoprenoid distributions. Chem Geol 206:231–248

Schwark L, Ruebsam W (2024) Climate cyclicity-controlled recurrent bottom-water ventilation events in the aftermath of the Toarcian Oceanic Anoxic Event: the Jenkyns Event. Int J Earth Sci (Geologische Rundschau). https://doi.org/10.1007/s00531-024-02417-7

Senglaub Y, Brix MR, Adriasola AC, Littke R (2005) New information on the thermal history of the southwestern Lower Saxony Basin, northern Germany, based on fission track analysis. Int J Earth Sci 94:876–896

Song J, Littke R, Weniger P (2017) Organic geochemistry of the lower Toarcian Posidonia Shale in NW Europe. Org Geochem 106:76–92

Storm MS, Hesselbo SP, Jenkyns HC, Ruhl M, Ullmann CV, Xu W, Leng MJ, Riding JB, Gorbanenko O (2020) Orbital pacing and secular evolution of the Early Jurassic carbon cycle. Proc Nat Acad Sci 117(8):3974–3982

Storm MS, Hesselbo SP, Jenkyns HC, Ruhl M, Al-Suwaidi AH, Percival LM, Mather TA, Damborenea SE, Manceñido MO, Riccardi AC (2024) Integrated stratigraphy of Pliensbachian and Toarcian strata from the northern Neuquén Basin, Argentina. Newsletters on Stratigraphy: in press

Suan G, Nikitenko BL, Rogov MA, Baudin F, Spangenberg JE, Knyazev VG, Glinskikh LA, Goryacheva AA, Adatte T, Riding JB, Föllmi KB, Pittet B, Mattioli E, Lécuyer C (2011) Polar record of Early Jurassic massive carbon injection. Earth Planet Sci Lett 312:102–113

Suan G, van De Schootbrugge B, Adatte T, Fiebig J, Oschmann W (2015) Calibrating the magnitude of the Toarcian carbon cycle perturbation. Paleoceanography 30:495–509

Svensen HH, Planke S, Chevallier L, Malthe-Sørenssen A, Corfu F, Jamtveit B (2007) Hydrothermal venting of greenhouse gases triggering Early Jurassic global warming. Earth Planet Sci Lett 256:554–566

Sweere T, van den Boorn S, Dickson AJ, Reichart G-J (2016) Definition of new trace-metal proxies for the controls on organic matter enrichment in marine sediments based on Mn Co, Mo and Cd concentrations. Chem Geol 441:235–245

Them TR, Gill BC, Caruthers AH, Gröcke DR, Tulsky ET, Martindale RC, Poulton TP, Smith PL (2017) High-resolution carbon isotope records of the Toarcian Oceanic Anoxic Event (Early Jurassic) from North America and implications for the global drivers of the Toarcian carbon cycle. Earth Planet Sci Lett 459:118–126

Them TR, Gill BC, Caruthers AH, Gerhardt AM, Gröcke DR, Lyons TW, Marroquín SM, Nielsen SG, Trabucho Alexandre JP, Owens JD (2018) Thallium isotopes reveal protracted anoxia during the Toarcian (Early Jurassic) associated with volcanism, carbon burial, and mass extinction. PNAS 115:6596–6601

Thibault N, Ruhl M, Korte C, Ullmann CV, Kemp DB, Gröcke DR, Hesselbo SP (2018) The wider context of the Lower Jurassic Toarcian oceanic anoxic event in Yorkshire coastal outcrops, UK. Proc Geol Assoc 129:372–391

Ullmann CV, Boyle B, Duarte LV, Hesselbo SP, Kasemann S, Klein T, Lenton T, Piazza V, Aberhan M (2020) Warm afterglow from the Toarcian Oceanic Anoxic Event drives the success of deep-adapted brachiopods. Sci Rep 10:6549

van Breugel Y, Baas M, Schouten S, Mattioli E, Sinninghe-Damsté JS (2006) Isorenieratane record in black shales from the Paris Basin, France: constraints on recycling of respired CO_2 as a mechanism for negative carbon isotope shifts during the Toarcian oceanic anoxic event. Paleoceanography 21:PA4220. https://doi.org/10.1029/2006PA001305

van de Schootbrugge B, Little CTS, Püttmann W, Guex J, Fraguas A, Wonik T, Blau T, Pross J, van der Weijst CMH, Wignall PB, Luppold FW, Oschmann W, Hunze S, Richoz S, Herrle JO, Meister C, Fiebig J, Suan G (2019) The Schandelah Scientific Drilling Project: a 25-million year record of Early Jurassic palaeoenvironmental change from northern Germany. Newsl Stratigr 52:249–296

Vandenbroucke M, Behar F, San Torcuato A, Rullkotter J (1993) Kerogen maturation in a reference kerogen Type II series: the Toarcian shales of the Hils syncline. NW Germany Org Geochem 20(7):961–972

Voigt E (1968) Über Hiatus-Konkretionen (dargestellt an Beispielen aus dem Lias). Geol Rundsch 58:281–296

Wetzel A, Allia V (2000) The significance of hiatus beds in shallow-water mudstones: an example from the Middle Jurassic of Switzerland. J Sediment Res 70:170–180

Woodfine RG, Jenkyns HC, Sarti M, Baroncini F, Violante C (2008) The response of two Tethyan carbonate platforms to the early Toarcian (Jurassic) oceanic anoxic event: environmental change and differential subsidence. Sedimentology 55:1011–1028

Xu W, Ruhl M, Jenkyns HC, Hesselbo SP, Riding JB, Selby D, Naafs BDA, Weijers JW, Pancost RD, Tegelaar EW, Idiz EF (2017) Carbon sequestration in an expanded lake system during the Toarcian oceanic anoxic event. Nat Geosci 10:129–134

Xu W, Ruhl M, Jenkyns HC, Leng MJ, Huggett JM, Minisini D, Ullmann CV, Riding JB, Weijers JW, Storm MS, Percival LM, Tosca NJ, Idiz EF, Tegelaar EW, Hesselbo SP (2018a) Evolution of the Toarcian (Early Jurassic) carbon-cycle and global climatic controls on local sedimentary processes (Cardigan Bay Basin, UK). Earth Planet Sci Lett 484:396–411

Xu W, Mac Niocaill C, Ruhl M, Jenkyns HC, Riding JB, Hesselbo SP (2018b) Magnetostratigraphy of the Toarcian Stage (Lower Jurassic) of the Llanbedr (Mochras Farm) Borehole, Wales: basis for a global standard and implications for volcanic forcing of palaeoenvironmental change. J Geol Soc 175:594–604

Ziegler PA (1992) Geological Atlas of Western and Central Europe, 2nd edn. Geological Society of London, London